*Published in: Molecular Endocrinology (2004), vol. 18, iss. 10, pp. 2522-2542*
*Status: Postprint (Author's version)*


# Cathepsin D Processes Human Prolactin into Multiple 16K-Like N-Terminal Fragments: Study of Their Antiangiogenic Properties and Physiological Relevance

DAVID PIWNICA, PHILIPPE TOURAINE, INGRID STRUMAN, SEBASTIEN TABRUYN, GERARD BOLBACH, CARMEN CLAPP, JOSEPH A. MARTIAL, PAUL A. KELLY, and VINCENT GOFFIN

*Institut National de la Santé et de la Recherche Medicale (INSERM) Unit 584 (D.P., P.T., P.A.K., V.G.), Hormone Targets, Faculté de Médecine Necker, 75730, Paris Cedex 15, France; Laboratory of Molecular Biology and Genetic Engineering (I.S., S.T., J.A.M.), University of Liege, B-4000, Sart Tilman, Belgium; Laboratoire de Chimie Structurale Organique et Biologique (G.B.), Université Pierre et Marie Curie, 75252, Paris Cedex 05, France; and Neurobiology Institute (C.C.), National Autonomous University of Mexico, Queretaro, Mexico 76230*

**Abstract:** 16K prolactin (PRL) is the name given to the 16-kDa N-terminal fragment obtained by proteolysis of rat PRL by tissue extracts or cell lysates, in which cathepsin D was identified as the candidate protease. Based on its antiangiogenic activity, 16K PRL is potentially a physiological inhibitor of tumor growth. Full-length human PRL (hPRL) was reported to be resistant to cathepsin D, suggesting that antiangiogenic 16K PRL may be physiologically irrelevant in humans. In this study, we show that hPRL can be cleaved by cathepsin D or mammary cell extracts under the same conditions as described earlier for rat PRL, although with lower efficiency. In contrast to the rat hormone, hPRL proteolysis generates three 16K-like fragments, which were identified by N-terminal sequencing and mass spectrometry as corresponding to amino acids 1-132 (15 kDa), 1-147 (16.5 kDa), and 1-150 (17 kDa). Biochemical and mutagenetic studies showed that the species-specific digestion pattern is due to subtle differences in primary and tertiary structures of rat and human hormones. The antiangiogenic activity of N-terminal hPRL fragments was assessed by the inhibition of growth factor-induced thymidine uptake and MAPK activation in bovine umbilical endothelial cells. Finally, an N-terminal hPRL fragment comigrating with the proteolytic 17-kDa fragment was identified in human pituitary adenomas, suggesting that the physiological relevance of antiangiogenic N-terminal hPRL fragments needs to be reevaluated in humans.

**Abbreviations:** bFGF, Basic fibroblast growth factor; BUVEC, bovine umbilical vein endothelial cells; FCS, fetal calf serum; GRO, growth-related oncogene; hPRL, human PRL; mAb, monoclonal antibody; MALDI-TOF, matrix-assisted laser desorption/ionization time-of-flight; MCP, monocyte chemotactic protein; PRL, prolactin; 16K PRL, 16-kDa fragment of PRL; rPRL, rat PRL; TIMP, tissue inhibitor of metalloproteinase; VEGF, vascular endothelial growth factor; WT, wild-type.

## INTRODUCTION

THE NAME 16 K PROLACTIN (PRL) was given 15 yr ago to the 16-kDa fragment resulting from the *in vitro* proteolysis of full-length rat PRL (rPRL) (23 kDa) by cell lysates or tissue extracts (e.g. 25,000 x *g* pellet of rat mammary gland) under acidic conditions (1, 2). Purified 16K rPRL was subsequently demonstrated to exert antiangiogenic properties in various *in vitro* and *in vivo* models (3), which confers potential antitumor potency to this polypeptide. These findings have considerably increased the interest of the scientific community for 16K PRL, and several investigations have been performed since its discovery to elucidate the molecular mechanisms underlying its interesting biological properties.

The generation of rat 16K PRL *in vitro* requires two steps (2). First, efficient proteolysis requires acidic pH (<4), in agreement with the fact that the candidate protease involved, cathepsin D (4), is an acidic protease. Two cleavage sites were identified in rPRL, following residues 145 and 148 (4, 5). Because all PRLs contain an internal disulfide bond between cysteines 56 and 172 (rat sequence numbering) (6), the proteolysis step generates so-called cleaved PRL, a PRL isoform in which N-terminal 16-kDa (residues 1-145) and C-terminal 7-kDa (residues 149-197) fragments remain covalently linked. The release of the 16-kDa fragment thus requires a second step, *i.e.* the reduction of cleaved PRL (Fig. 1). To circumvent the difficulties linked to the purification of 16K PRL from PRL proteolysed by tissue extracts, 16K PRL was subsequently produced by recombinant

technology using the human PRL (hPRL) sequence. Several versions of recombinant 16K-like hPRL were generated depending on the position of the engineered stop codon inserted within the hPRL cDNA sequence (7). Recombinant hPRL fragments encompassing sequences 1-124 (8) and 1-139 and 1-142 (9) were engineered, and all of these were shown to display antiangiogenic properties similar to those reported for rat 16K PRL in various bioassays. Using the 1-139 hPRL fragment, some of the molecular mechanisms underlying the antiangiogenic activity of N-terminal PRL fragments were determined. For example, 16K PRL was shown to inhibit the mitogenic activity of vascular endothelial growth factor (VEGF) or basic fibroblast growth factor (bFGF) on endothelial cells, an effect involving the inhibition of signaling pathways triggered by these angiogenic factors (10, 11). In addition to this inhibitory action of growth factors, 16K PRL intrinsically induces apoptosis by activating the caspase pathway via nuclear factor κB (12,13) and the expression of plasminogen activator inhibitor-1, a specific inhibitor of urokinase that activates proteases involved in endothelial cell migration and tissue remodeling (14). All these effects are presumably mediated by a membrane receptor that differs from the classical PRL receptor, but remains to be identified (15).

Based on its antiangiogenic properties, 16K PRL appears to be a new candidate in the wide spectrum of antitumor drugs. But maybe more importantly, because full-length (23K) and 16K PRLs were recently proposed to have opposing actions on angiogenesis in experimental models (the former stimulates, the latter inhibits) (9), the possibility exists that their respective ratio may participate in the physiological regulation of angiogenesis *in vivo*, especially in the context of PRL-secreting tumors (16). In addition, because full-length PRL exerts proliferative actions in various models of breast tumors (17), the existence of antiangiogenic N-terminal 16K-like fragments of hPRL that may balance the effect of PRL on tumor growth *in vivo* is a question that deserves further investigation. Several years ago, one of us reported that very little specific cleavage products could be obtained after incubation of hPRL with mammary subcellular fractions (2). In good agreement, the group of Ben-Jonathan (18) reported in 1999 that hPRL was resistant to cleavage by cathepsin D or mammary cell extracts at acidic pH. In contrast, these authors showed that thrombin can process hPRL at physiological pH into a 16-kDa fragment, but the latter was identified as the C-terminal end of the hormone (sequence 54-199) and was shown to be devoid of any angiostatic properties (18). Based on that study, any human homolog to the antiangiogenic 16-kDa fragment obtained with rPRL wou Id be irrelevant.

Closer analysis of the data provided by Ben-Jonathan and colleagues prompted us to reevaluate the proteolysis of hPRL into N-terminal 16K-like fragments. The present study is the first report showing the ability of hPRL to be cleaved by normal and tumor mammary cell extracts into a pattern of multiple fragments, specific to the human species and distinct from the pattern observed with the rat hormone. At least four cleavage sites by the acidic protease cathepsin D were identified within hPRL sequence, three of which generate N-terminal 16K-like fragments that all display antiangiogenic activity. These observations clearly renew the interest for studying the potential relevance of antiangiogenic 16K-like PRL in human species.

## RESULTS

### The Pattern of PRL Fragments Generated by Human Breast Cells Is Species Specific

Many tissue extracts, including mammary gland, liver, or prostate, were previously shown to process rPRL into 16K PRL in acidic conditions (19); therefore we used mammary epithelial cells to study the proteolysis of hPRL Electrophoresis under reducing conditions reveals that acidified T-47Dco cell lysates cleave hPRL into multiple fragments the apparent molecular masses of which were estimated to be approximately 17, 15, and 11 kDa based on their electrophoretic mobility, the two larger clearly differing in size from the formerly described 16K rPRL (Fig. 1A, *right panel).* Smaller fragments of approximately 8 and 5 kDa could also be seen, although their size made detection more difficult (data not shown). Electrophoresis under non-reducing conditions (Fig. 1A, *left panel)* indicates that rat and human PRL fragments remain linked by intramolecular disulfide bonds because only intact oxidized PRL (23 kDa) and slower migrating cleaved form(s) of PRL were detected, the latter appearing as a single band (rat) or as a doublet (human). These observations confirm pioneering experiments investigating hPRL proteolysis by subcellular fractions of mammary gland (2).

The various bands detected in Coomassie blue staining were clearly identified as hPRL fragments by immunoblotting with the anti-hPRL monoclonal antibody (mAb) (6E4) directed against recombinant 16K hPRL (Fig. 1B). In certain experiments, the larger band (referred to as 17K PRL) detected by Coomassie blue staining appeared to contain two immunoreactive bands corresponding to molecular masses of approximately 16.5/17 kDa (Fig. 1B). Because of almost identical electrophoretic mobilities, these two fragments frequently focused as a single band. A similar pattern of hPRL fragments, with 17- and 15-kDa fragments predominantly detected, was obtained when hPRL was digested using conditioned medium obtained from T47Dco cultures (Fig. 1C),

indicating that the protease involved is secreted by the cells. Proteolysis occurred only in acidic conditions, suggesting the involvement of an acidic protease. The absence of cleavage when using heated conditioned medium (Fig. 1C) or cell lysates (data not shown) demonstrates that hPRL does not undergo spontaneous degradation during the assay. Finally, 17-kDa and, to a much lesser extent, 15-kDa fragments comigrating with those generated using T47Dco lysates (data not shown) were also obtained when digestion was performed using acidified tissue homogenates from human breast biopsies, obtained from either normal or tumor tissue (Fig. 1D). Although the cleavage efficiency differed from one breast biopsy to another, the number of samples available for these preliminary studies was insufficient to state that the proteolytic efficiency is related to the pathophysiological status of the tissue (tumor *vs.* normal). However, this experiment indicates that hPRL proteolysis is not limited to the T47Dco cell line.

Taken together, our data are in good agreement with one of our previous reports (2) and indicate that 1) hPRL can be processed into several fragments by an acidic protease expressed in mammary cells and se-

creted into the extracellular space, and 2) the proteolytic pattern is specific to the human hormone and distinct from the well-known 16K rPRL.

**Fig. 1:** *Cleavage of hPRL by Human Mammary Cell Lysates or Conditioned Medium*

Rat and human PRL were digested in various conditions (as indicated) by T47Dco cell lysates (A and B), T47Dco conditioned medium (C), or cell extracts of tumor and normal human breast (D). All SDS-PAGE gels were run under reducing conditions, except in *left panel A*, and immunoblots were performed using monoclonal anti-hPRL 6E4. cl-PRLs, Cleaved PRLs

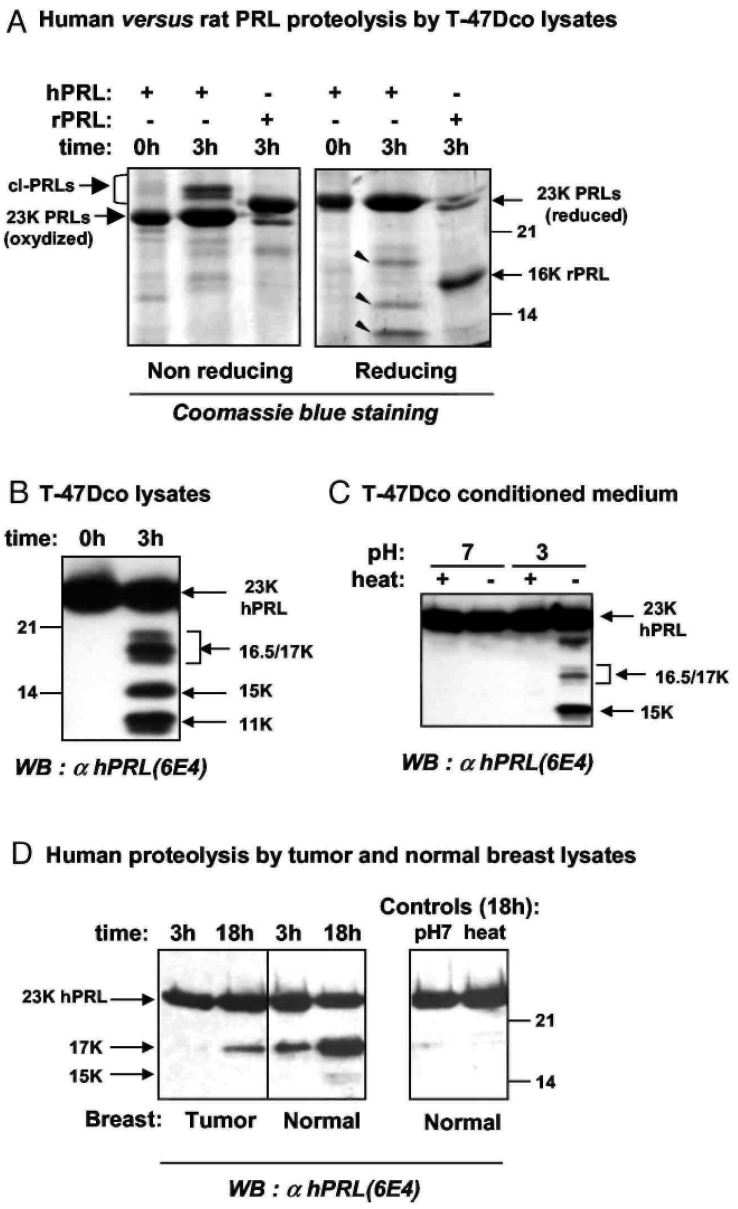


**The Candidate Protease Involved in hPRL Cleavage Is Cathepsin D**

We then tried to identify the protease involved, first by using various protease inhibitors. Cleavage of hPRL by T-47Dco conditioned medium was inhibited in the presence of pepstatin or EDTA, but not of the other inhibitors tested (Fig. 2A). Because pepstatin in known to inhibit cathepsin D, the involvement of this protease in hPRL cleavage was further examined, although it was claimed that hPRL is resistant to cathepsin D (18). First, incubation of acidified T-47Dco conditioned medium with a neutralizing anticathepsin D antibody before addition of hPRL prevents any proteolysis, strongly supporting the pivotal role of this protease in the cleavage (Fig. 2B). Second, the pattern of hPRL fragments generated by purified human cathepsin D appears to be virtually identical to that obtained using T47Dco cell lysates (Fig. 2C), *i.e.* characteristic of human species (see Fig. 1). The proteolytic profile of pituitary-purified hPRL was found to be identical to that obtained with recombinant PRL, demonstrating that the present findings are not due to the fact that we use bacterially produced hPRL for the proteolysis studies (Fig. 2D). Finally, hPRL proteolysis performed using thrombin (Fig. 2E), a protease that was shown to process hPRL into a C-terminal 16-kDa fragment (18), unequivocally demonstrated that none of the 15- to 17-kDa fragments generated by cathepsin D match the C-terminal 16K hPRL

Taken together, these results indicate that 1) under acidic conditions, the aspartyl protease cathepsin D is able to cleave hPRL into several fragments distinct from the well-characterized 16K rPRL, and 2) this protease is the

candidate protease responsible for hPRL processing by mammary cell extracts or conditioned media.

**Composition of hPRL Fragments**

The composition of hPRL fragments was determined using three complementary approaches: proteolysis experiments using N-terminal-deleted hPRL mutants, N-terminal sequencing, and mass spectrometry. When hPRL analogs lacking the nine or 14 N-terminal residues (20) were used for cathepsin D-mediated proteolysis, the electrophoretic mobility of the four larger bands (17, 16.5, 15, and 11 kDa) was accelerated, suggesting they are indeed N-terminal fragments (data not shown). In a second experiment, hPRL was digested using T47Dco cell lysates or purified cathepsin D, and immunoreactive bands were recovered from anti-hPRL immunoblots for N-terminal sequencing analysis. The 17K/16.5K (not separated) and 15K peptides share the same N-terminal sequence as undigested recombinant hPRL (with the additional initiation methionine) (21), confirming that they correspond to N-terminal fragments (Fig. 3A). Identical N-terminal sequences were obtained for cognate hPRL fragments resulting from digestion by mammary cell lysates or by purified cathepsin D, strengthening the likelihood that the latter is the cellular protease involved. The 8-kDa and 5-kDa fragments start at residues $Ile_{133}$ and $Ser_{151}$, respectively, suggesting they may be complementary to 15K and 16.5K/17K hPRL The 11-kDa fragment appeared to contain more than a single peptide, because signals starting at residue 1 and $Ile_{87}$ were detected. A minor signal starting at $Phe_{37}$ was also detected within the 8-kDa band.

To determine the exact composition of these hPRL fragments, we performed matrix-assisted laser desorption/ionization (MALDI) time-of-flight (TOF) mass spectrometry analysis using a solution of hPRL digested by cathepsin D. All analyses were performed in parallel using two hPRL analogs the molecular mass of which differs from that of WT hPRL, namely Δ1-9-hPRL (lacking residues 1-9) (20) and G129R-hPRL (Arg substituted for $Gly_{129}$) (22). To unambiguously distinguish peaks corresponding to hPRL fragments from background, we compared digested hPRL (WT and analogs) before and after reduction, because release of proteolytic fragment only occurs under reducing conditions (see *Introduction*). The experimental data of PRL-related ion peaks and the theoretical molecular weights corresponding to the candidate sequences are reported in Table 1. Based on their molecular masses, the three peaks detected in the 15- to 17-kDa range after proteolysis of WT hPRL (Fig. 3B) were assigned to sequences 1-132, 1-147, and 1-150, in perfect agreement with the fact that corresponding peaks were all shifted toward smaller masses (by ~800 Da) when proteolysis involved the Δ1-9-hPRL analog, and toward higher masses (by ~100 Da) when proteolysis involved G129R-hPRL (Table 1). Two other peaks (5.7 and 7.9 kDa) remained unchanged whether proteolysis was performed using WT hPRL, Δ1-9-hPRL, or G129R-hPRL, indicating they correspond to C-terminal sequences that could be assigned to fragments 133-199 and 151-199, respectively. Finally, two clusters of peaks assigned to sequences 1-80, 1-84, and 1-85 for the first, and 85-199, 88-199, and 90-199 for the second were also detected in the 9- and 13-kDa regions of the spectra, respectively (data not shown). In agreement with the sequences assigned, the first cluster was shifted to smaller masses for Δ1-9-hPRL but remained unchanged for G129R-hPRL, whereas it was the opposite for the second cluster. These fragments presumably result from initial cleavage around residue 85 and subsequent aminopeptidase and carboxypeptidase activities.

**Fig. 2:** *The Mammary Protease Involved in hPRL Cleavage Is Cathepsin D*
Proteolysis of hPRL was performed by conditioned medium or cell lysates of T-47Dco, or purified proteases as indicated in *Materials and Methods.* A, Among the various protease inhibitors tested, only EDTA and pepstatin inhibit proteolysis by conditioned medium. B, Immunodepletion of conditioned medium by anticathepsin D antibody (8 μg/ml) prevents hPRL cleavage. C, Proteolysis of hPRL by T-47Dco lysates or purified human cathepsin D generates a similar pattern of hPRL fragments. D, The proteolytic pattern obtained with cathepsin D is identical whether recombinant or pituitary-purified hPRL is used. E, The proteolytic patterns of hPRL resulting from digestion by cathepsin D and thrombin are different.

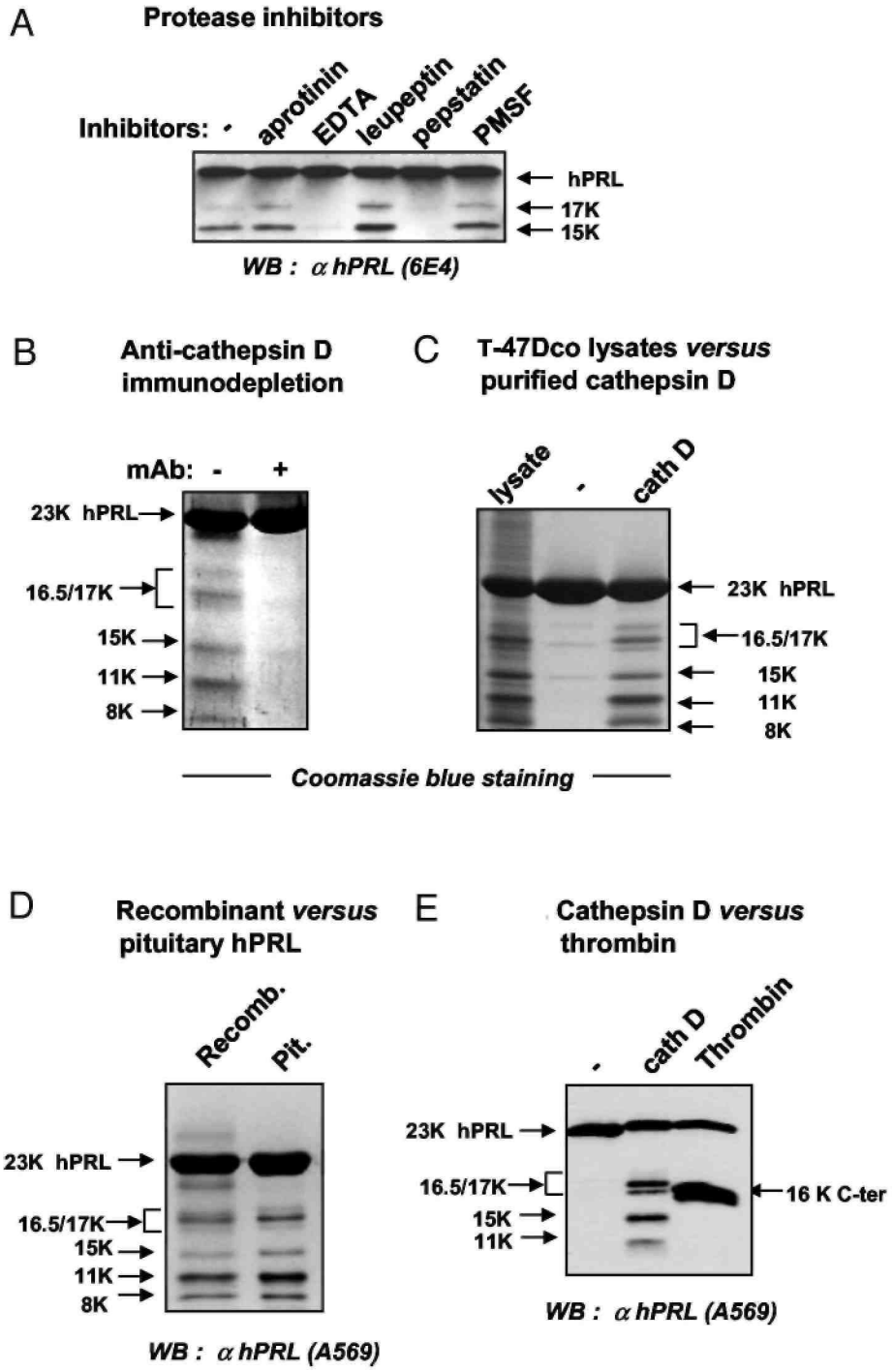


Taken together, these results obtained by *in vitro* proteolysis of hPRL analogs, N-terminal sequencing, and mass spectrometry analyses indicate that hPRL contains at least four cleavage sites for cathepsin D (Fig. 3, C and D). The three sites generating 16K-like N-terminal fragments are unambiguously located between residues 132-133, 147-148, and 150-151. The location of the fourth site is less clear and is presumably located near residue 85.

**Fig. 3:** *Composition of hPRL Fragments Generated by Human Breast Cells*
A, hPRL fragments generated by T-47Dco lysates or purified cathepsin D (see Fig. 2C) were sequenced at their N-terminal end (the initiation methionine of recombinant hPRL is omitted for clarity). Corresponding fragments in both digestion have identical N termini. Minor sequences were obtained for the 11- and 8-kDa bands (*see Results).* B, Mass spectrometry analysis of hPRL was performed before (*upper panels)* and after (*lower panels)* reduction. Only the data corresponding to the three N-terminal 15- to 17K fragments are shown. The peaks appearing in reduced samples correspond to hPRL fragments released from cleaved hPRL. C indicates the peak of the calibrant. C, Schematic representation of the four cleavage sites for cathepsin D in hPRL, as deduced from N-terminal sequencing and mass spectrometry. D, As recently confirmed by NMR (41), hPRL adopts the four-helix bundle folding (helices are numbered 1-4). The four cathepsin D

cleavage sites that we identified in this study are located in the same region of the folded protein (*dotted circle).* For each site, the main chain atoms of the amino acids before and after the cleavage are represented (red, oxygen; *light blue*, carbon; *dark blue*, nitrogen).
*(Figure continues on next page.)*

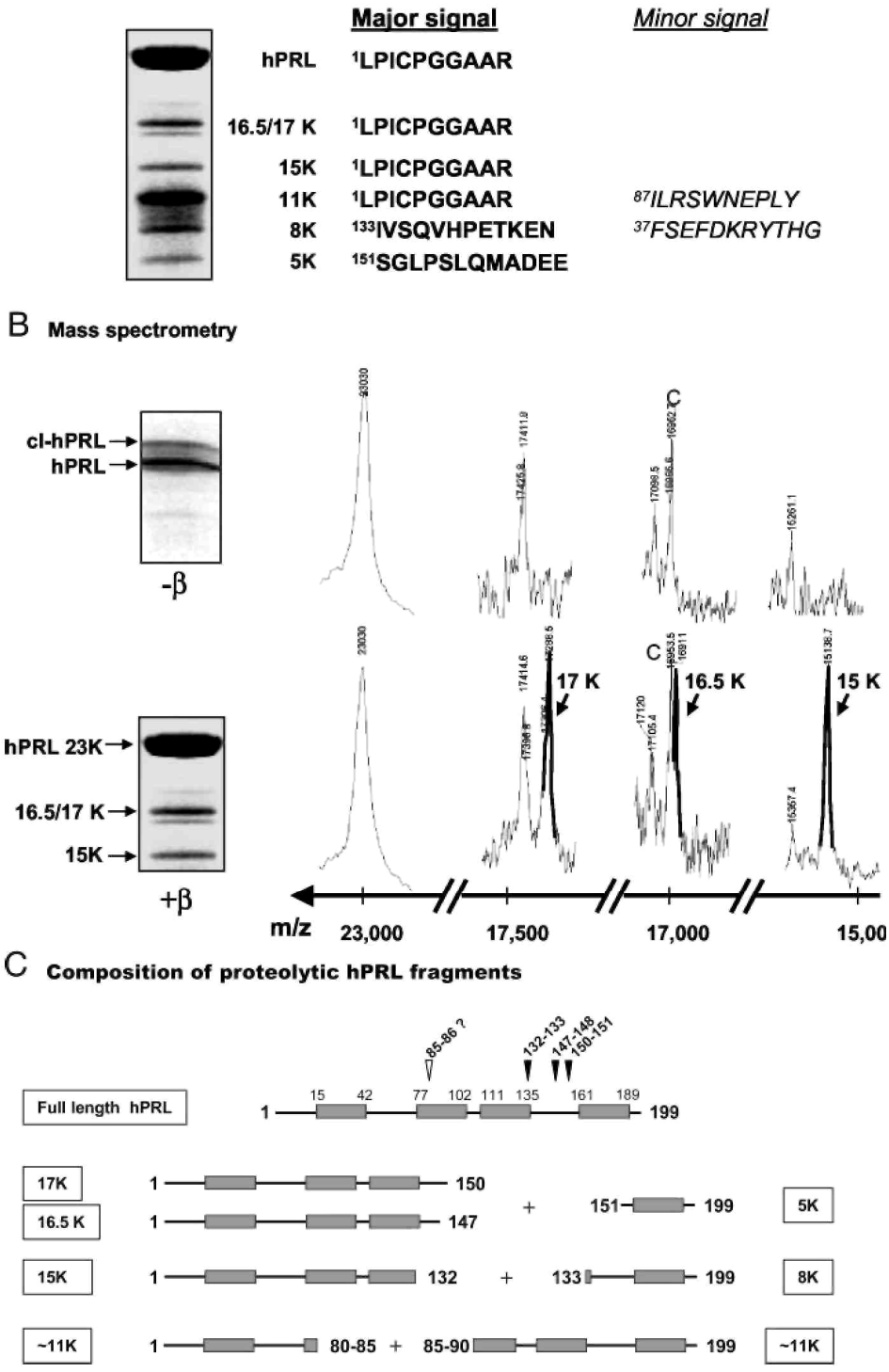

**Figure 3:** *Continued*

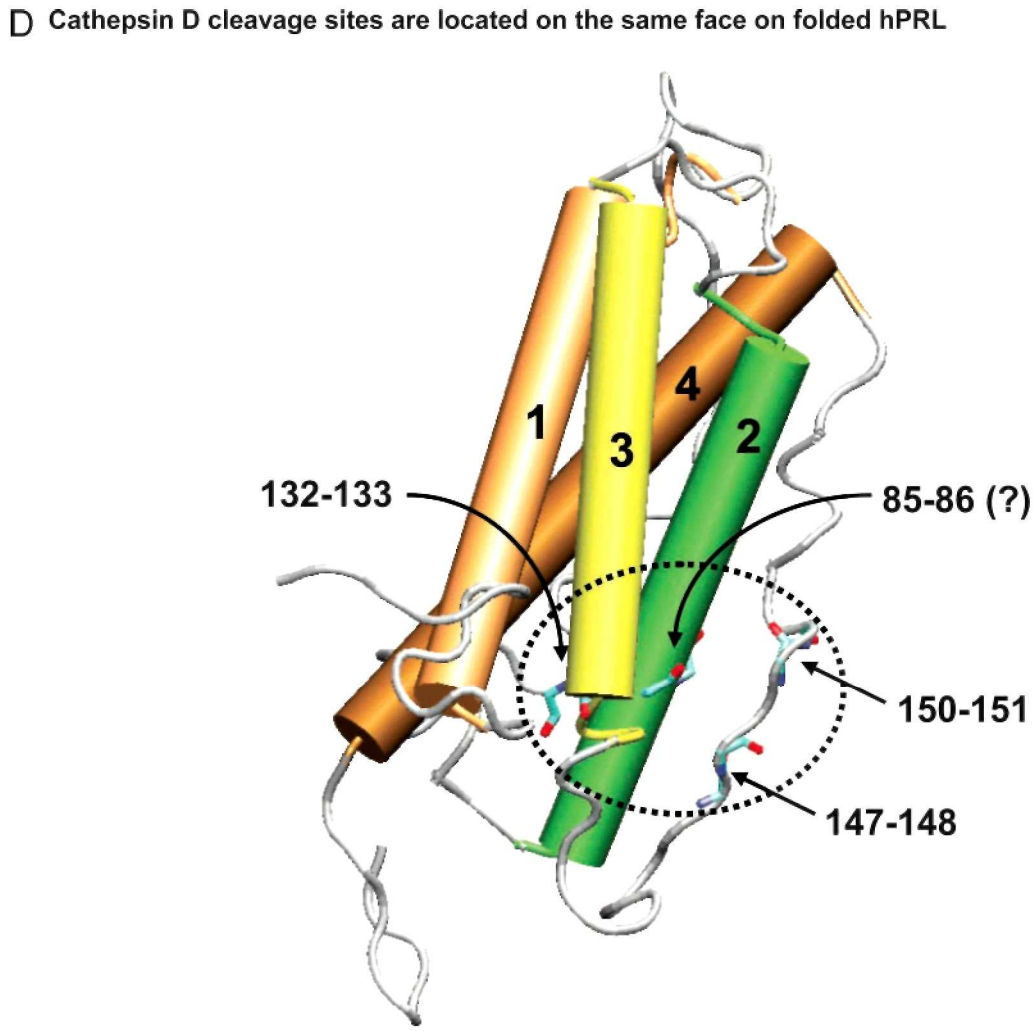


**Table 1:** *Theoretical and Experimental Molecular Weights (mw) of hPRL Fragments Identified by Mass Spectrometry*

| Sequence | WT hPRL | | Δ1-9 hPRL | | G129R-hPRL | |
|---|---|---|---|---|---|---|
| | Theoretical mw | Exp. $MH^+$ | Theoretical mw | Exp $MH^+$ | Theoretical mw | Exp $MH^+$ |
| Full length | 23,029.3 | 23,028 ± 3 | 22,233.4 | 22,238 ± 5 | 23,128.5 | 23,127 ± 3 |
| 1-132 | 15,136.3 | 15,138 ± 3 | 14,340.3 | 14,342 ± 4 | 15,235.4 | 15,235 ± 3 |
| 1-147 | 16,904.3 | 16,907 ± 3 | 16,108.3 | Not observed | 17,003.4 | Not observed |
| 1-150 | 17,286.7 | 17,289 ± 3 | 16,490.7 | 16,510 ± 4 | 17,385.9 | Not observed |
| 133-199 | 7,911.0 | 7,914 ± 3 | 7,911.0 | 7,913 ± 3 | 7,911.0 | 7,914 ±2 |
| 151-199 | 5,760.6 | 5,766 ± 3 | 5,760.6 | 5,763 ± 3 | 5,760.6 | 5,764 ± 3 |

The experimental value refers to the average mass of the protonated molecules of protein and fragments. Exp, Experiment.

**Species Specificity of PRL Proteolytic Pattern**

We next addressed the question whether the specific characteristics of hPRL proteolysis (cleavage efficiency and fragment pattern) could be correlated to any intrinsic features of its primary structure. Interestingly, alignment between rat and human sequences shows that the two cleavage sites identified in the rat hormone (4, 5) are topologically equivalent to those generating 16.5K and 17K hPRL (Fig. 4A), with release of a tripeptide corresponding to residues 146-148 in the rat and 148-150 in the human hormone. This indicates that 16.5K hPRL

is homologous to 16K rPRL, whereas 15K hPRL has no equivalent in the rat hormone. Two cathepsin D recognition sites within hPRL show major differences with the rat sequence, namely $Lys_{131}$ (rat)/$Leu_{133}$ (human) substitution in the first one, and $Leu_{146}$ (rat)/$Pro_{148}$ (human) substitution in the second (Fig. 4A). Four PRL mutants containing single amino acid substitutions at these positions were produced and analyzed (hPRL L132K, hPRL P148L, hPRL P148A and rPRL P146L). All analogs maintained full bioactivity in a hPRL receptor-mediated bioassay (23), suggesting that the mutations did not significantly affect protein folding (data not shown). Substitution of Leu (Fig. 4B, *left panel*) or Ala (data not shown) for $Pro_{148}$ in hPRL dramatically increases proteolysis efficiency, because almost 90% of full-length hormone disappeared after 3 h of *in vitro* enzymatic reaction [there was no spontaneous degradation in the absence of enzyme (data not shown)]. In contrast, substitution of Pro for $Leu_{146}$ in rPRL had the opposite effect, because a significant amount of full-length hormone remained undigested after 3 h (Fig. 4B, *right panel*). This clearly indicates that a proline residue at position 148 (naturally occurring in hPRL) is detrimental to high cleavage efficiency, whereas a Leu (naturally occurring in rPRL) is not mandatory. In addition, the Pro-Leu substitution also modifies the proteolytic pattern. In rPRL, only the 16.5K fragment resulting from cleavage at the 148-149 site is detected (Fig. 4B, *right*), indicating that the other cleavage site (145-146) is rendered nonfunctional by the proline substitution. As would be expected, because removal of $Pro_{148}$ in hPRL renders the 147-148 site highly functional, this leads to the preferential formation of 16.5K hPRL and the complementary 5K fragment (Fig. 4B). With respect to the 132-133 recognition site, substitution of a Lys for $Leu_{132}$ in hPRL abolishes the cleavage, as deduced from the absence of the 15K fragment (Fig. 4B), which suggests that a lysine residue at this position (as naturally occurring in rPRL) is detrimental to cathepsin D cleavage.

These data indicate that the specific features of hPRL proteolysis are directly linked to the presence of two key residues in its sequence: $Pro_{148}$ prevents high cleavage efficiency at 147-148 and 150-151 sites, and $Leu_{132}$, in contrast, is responsible for the additional cleavage at site 132-133.

**Fig. 4:** *Site-Directed Mutagenesis in Cathepsin D Cleavage Sites*
A, Comparison of primary structures of rat and human PRL around the three cleavage sites generating 16K-like N-terminal fragments. The two major differences are *boxed*. B, *In vitro* proteolysis of human and rat PRL analogs mutated within cleavage sites. Point mutations at positions corresponding to $Pro_{148}$ and $Leu_{132}$ markedly modify the proteolytic pattern of both PRLs.

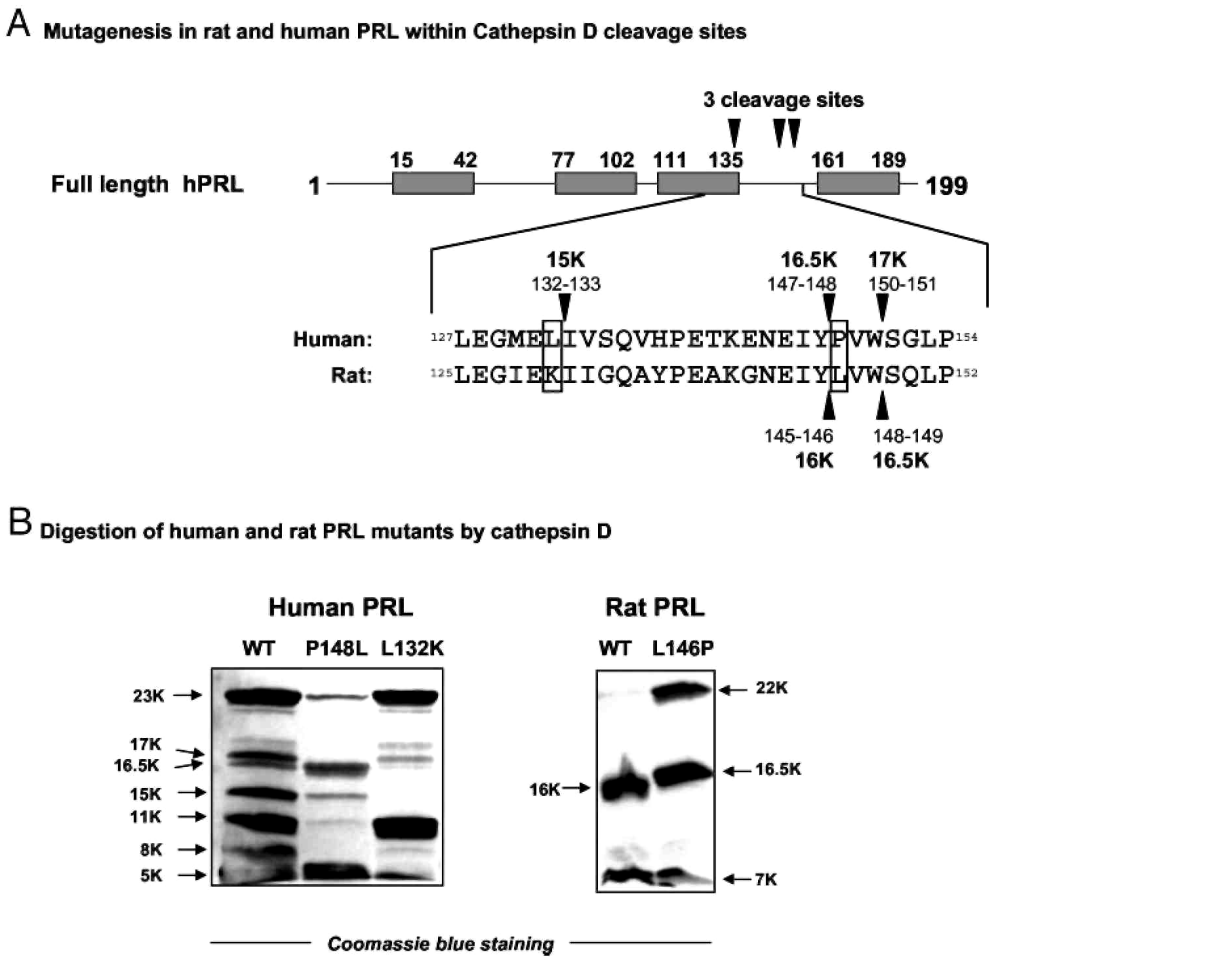

**Efficiency of hPRL Proteolysis by Cathepsin D**

We next investigated whether the moderate *in vitro* cleavage efficiency of hPRL was somehow linked to partly inappropriate experimental conditions of proteolysis. Although increasing the duration or the temperature of the enzymatic reaction led to the rapid disappearance of full-length hPRL (Fig. 5A, *left*), this failed to result in concomitant accumulation of proteolytic fragments, suggesting that these experimental conditions favor degradation rather than specific proteolysis. This phenomenon was not observed using rPRL (data not shown), suggesting it is hPRL specific. As would be expected, optimal proteolysis was observed between pH 3 and pH 4.5, and pH above 5.5 failed to generate any fragment (Fig. 5B).

To investigate whether some features of hPRL conformation could also participate in the moderate efficiency of cathepsin D cleavage, the proteolysis was performed in medium containing low concentrations of Triton X-100, with the goal of slightly relaxing the hormone structure (Fig. 5C). Interestingly, very low concentrations (0.01%) of detergent strongly increased cleavage efficiency (room temperature), and 0.05% Triton was sufficient to obtain near-complete proteolysis of hPRL with concomitant accumulation of proteolytic fragments. Because 0.05% Triton X-100 was detrimental to the cleavage of rPRL (data not shown), this suggests that at this concentration, the detergent modifies the folding of the hormone rather than increasing enzyme activity. Detergent concentrations above 0.1% were detrimental to hPRL proteolysis, presumably by affecting folding of the protease itself. In contrast to proteolysis performed at 37 C, which favors hPRL degradation (Fig. 5A), Triton X-100 led to the accumulation of 15K and 8K fragments. When the same experiment was performed using Δ1-9-hPRL analog, a slightly smaller fragment (~14 kDa) was obtained in place of the 15-kDa fragment observed after WT hPRL proteolysis (Fig. 5C), strongly suggesting that the detergent favors proteolysis at the 132-133 site, resulting in the generation of the N-terminal 15K fragment.

These experiments show that relaxing hPRL conformation using very low concentrations of Triton X-100 dramatically increases hormone processing at the 132-133 site.

**Fig. 5:** *Efficiency of hPRL Proteolysis by Cathepsin D*
A, Time course proteolysis of hPRL by cathepsin D at room temperature and 37 C. B, Efficiency of hPRL proteolysis over a 3-7 range of pH. C, Effect of various concentrations of Triton X-100 on proteolysis. Low concentration of the detergent (0.05%) enhances proteolysis without changing cleavage specificity, as demonstrated by the profile obtained for Δ1-9-hPRL. All SDS-PAGE were run under reducing conditions and gels were revealed using Coomassie blue staining.

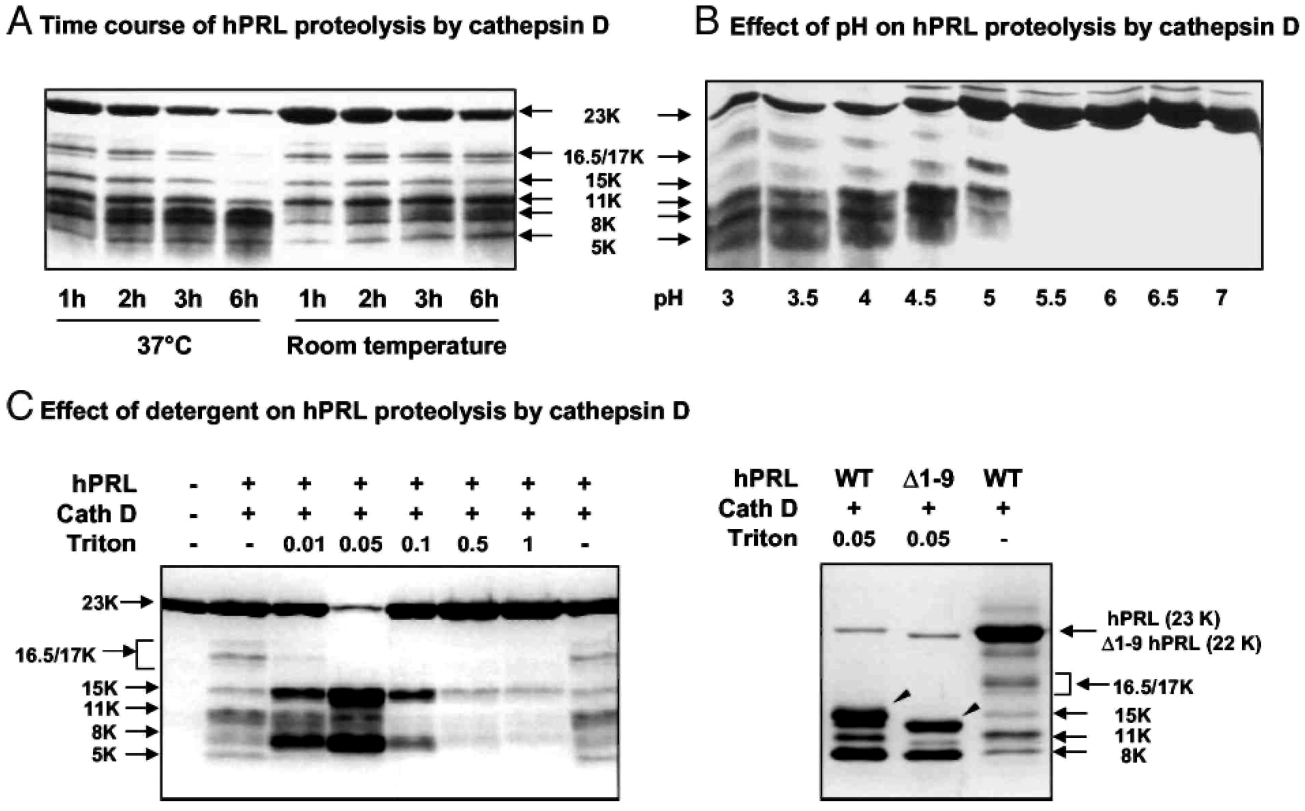

**Fig. 6:** *Expression of 15-17K hPRL Fragments in COS-7 Cells*

A, COS-7 cells were transfected with the indicated expression vectors, and conditioned media were harvested 24 h after transfection. The electrophoretic mobility of the various fragments under reducing conditions is correlated to their length. The *arrow* indicates the presence of a 16K-like fragment in conditioned medium from cells transfected with the expression plasmid of full-length hPRL. B, All fragments are expressed as three bands *(arrows)*, two of which correspond to glycosylated isoforms because a single band is obtained after treatment with glycosidase F. C, COS-7 cells secrete angiogenesis-related factors, some of which were identified using an angiogenesis antibody array (each antibody is *spotted in duplicate). Left panel* represents the negative control, obtained after incubation of the membrane array with DMEM/0.1% BSA. Spots A1, A2, and D8 are positive controls of the enhanced chemiluminescence reaction. Two angiogenesis-related factors were detected in fresh DMEM/0.1% BSA: IL-6 (B4), and TGFβ (C3), which probably result from small growth factor contamination in BSA (98% purity). *Right panel* shows a membrane that was incubated in DMEM/0.1 % BSA conditioned for 24 h with COS-7 cells. Five additional spots were detected, which correspond to bFGF (A8), GRO (B1), MCP-1 (B7), TIMP-2 (C5), and VEGF (C7) (see text).

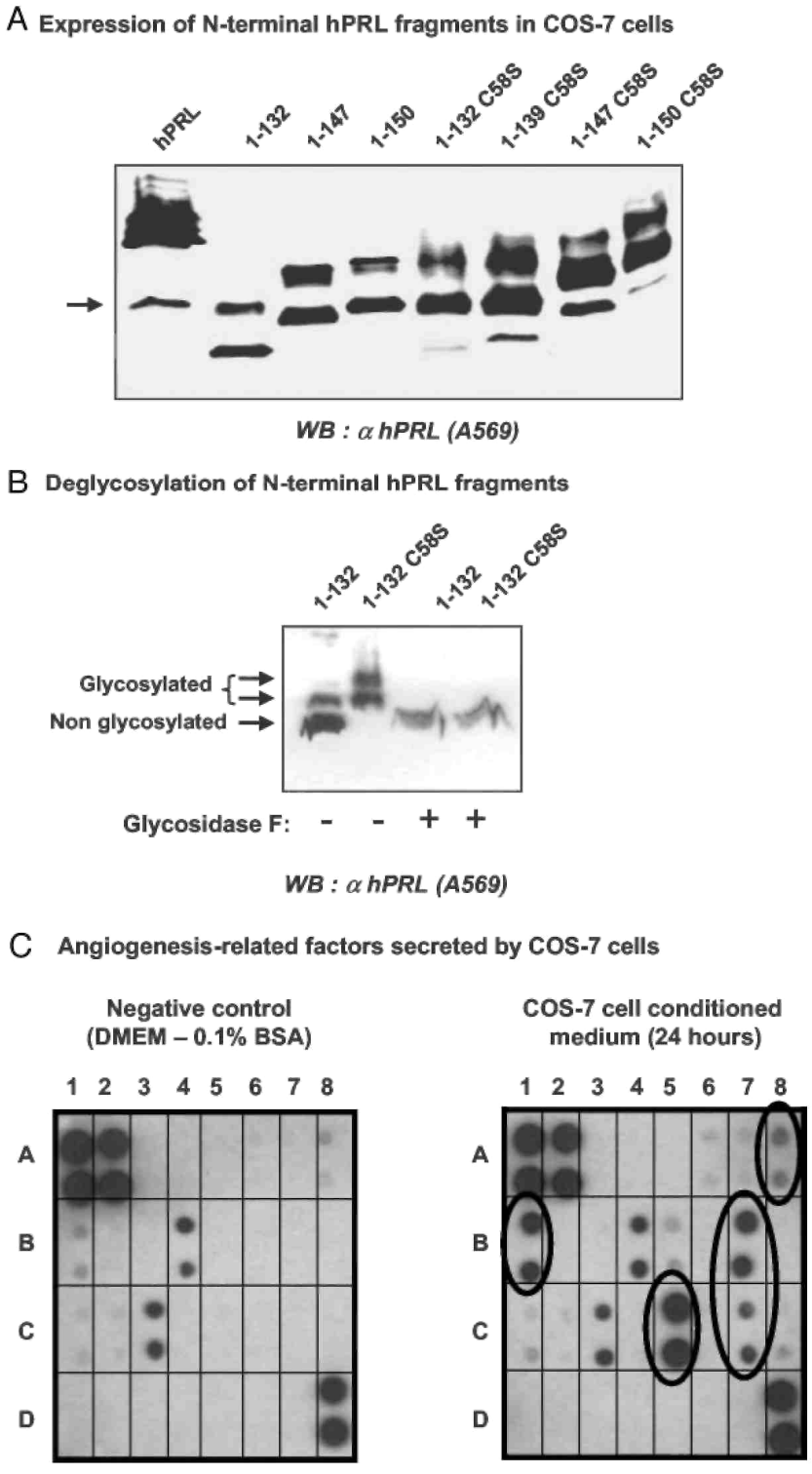

**Production of Recombinant N-Terminal Fragments of hPRL**

The next step of our investigations was to characterize the biological properties of the hPRL fragments identified. Due to both the moderate efficiency of hPRL cleavage in the absence of detergent and the physicochemical similarity of the three N-terminal hPRL fragments (size, charge), they could not be separated by standard chromatography. In addition, because chromatography steps are known to represent a potential source of endotoxin contamination (12), working with purified hormone can paradoxically be detrimental to the reliability of the results obtained in angiogenesis assays if the endotoxin issue is not under control. Therefore, we decided to produce recombinant hPRL fragments by transiently transfecting COS-7 cells, and then to stimulate endothelial cells directly with COS-7 cell-conditioned media, without any purification, to eliminate the risks of endotoxin contamination. This strategy has been successfully used in the past by us and others for similar purposes (24, 25).

To produce 15K, 16.5K, and 17K hPRL with a sequence strictly identical to that of the fragments generated by cathepsin D proteolysis and identified by mass spectrometry (Fig. 3B), a stop codon was inserted into the hPRL cDNA sequence at position 133, 148, or 151. To limit covalent oligomerization, we also produced the same fragments in which a Ser was substituted for free $Cys_{58}$, which normally forms an intramolecular disulfide bond with $Cys_{174}$ in full-length hPRL. As the positive control for bioassays, we produced in the same cell system the hPRL fragment encompassing residues 1-139 because this recombinant 16K hPRL construct was previously shown to exert antiangiogenic activity in various *in vitro* and *in vivo* bioassays (9,13, 25). As the negative controls, we transfected COS-7 cells with parental pc-DNA3.1 vector (mock transfection) or full-length hPRL vector, because hPRL is not expected to exert antiangiogenic activity.

hPRL fragments are expressed and secreted into the medium of transiently transfected COS-7 cells (Fig. 6A), and the absence of any immunoreactive band in conditioned medium of mock transfected cells (data not shown) confirmed that the bands detected are PRL related. As previously reported (26), N-terminal fragments were expressed in this system as two or three bands of different mobility. We demonstrated that the slower bands correspond to glycosylated iso-forms because a single band was obtained after analytical deglycosylation (Fig. 6B). Interestingly, the fragments containing the C58S were more glycoslytated than those containing the natural $Cys_{58}$, as previously observed (26).

The expression level of N-terminal fragments was usually lower (>1 order of magnitude) compared with full-length hPRL (Fig. 7C). This was not concomitant with an accumulation of hPRL fragments inside the cell (data not shown), suggesting that retention within the endoplasmic reticulum due to protein misfolding (27) does not explain the lower expression level. We also observed that the difference between expression of full-length and hPRL fragment was less pronounced when using freshly prepared plasmids, but this remains unexplained. Full-length hPRL secreted into the conditioned medium was quantified using a commercial ELISA specifically recognizing WT hPRL (28), and its concentration was in the range of 1-2 µg/ml. None of the N-terminal fragments could be detected in this ELISA, because the coated antibody (mAb 5601) was shown in this study to map a C-terminal hPRL epitope, absent in the fragments (see Fig. 9 below). The latter were thus quantified by densitometric analysis of autoradiographies taking 23-kDa hPRL as the reference. To take into account the relative production yields of full-length hormone *vs.* fragments, we routinely diluted the conditioned medium containing 23-kDa hPRL for functional assays (see legends to figures).

**Fig. 7:** *Antiangiogenic Activity of N-Terminal Fragments on BUVEC*

A, Dose-response activity of bFGF and COS-7 conditioned medium (transfected with parental pcDNA3.1) on thymidine uptake by BUVEC. This experiment indicates that growth factors secreted by COS-7 cells are able to induce thymidine uptake by BUVEC. B, Antiangiogenic activity of N-terminal hPRL fragments containing natural $Cys_{58}$ or mutated $Ser_{58}$. The figure represents the effect of 10 $\mu$l of conditioned medium in final volume of 200 $\mu$L. C, Dose-response activity of the three N-terminal hPRL fragments 15K, 16.5K, and 17K, containing $Cys_{58}$. The amounts of PRL hormones contained in the conditioned media used for this experiment are shown on the blot. As indicated in the text, conditioned medium containing hPRL was initially diluted 10- or 100-fold (panels B and C) to test similar amounts of protein for full-length and PRL fragments. Each panel is from a single experiment performed in triplicate and is representative of at least three similar experiments, performed with conditioned media obtained after different transfections. D, 16.5K hPRL fragment was removed from conditioned medium by immunoprecipitation using a polyclonal α-hPRL antibody (*right lane* on the blot, Ab+). Control sample was treated the same way except that the antibody was omitted in the immunoprecipitation (*left lane* on the blot, $Ab^-$). Immunodepleted conditioned medium ($Ab^+$, 6 $\mu$l) failed to inhibit thymidine incorporation by BUVEC (100% corresponds to the stimulation obtained with 6 µl mock-transfected conditioned medium). *Bars* represent averaged values from one experiment performed in triplicate.

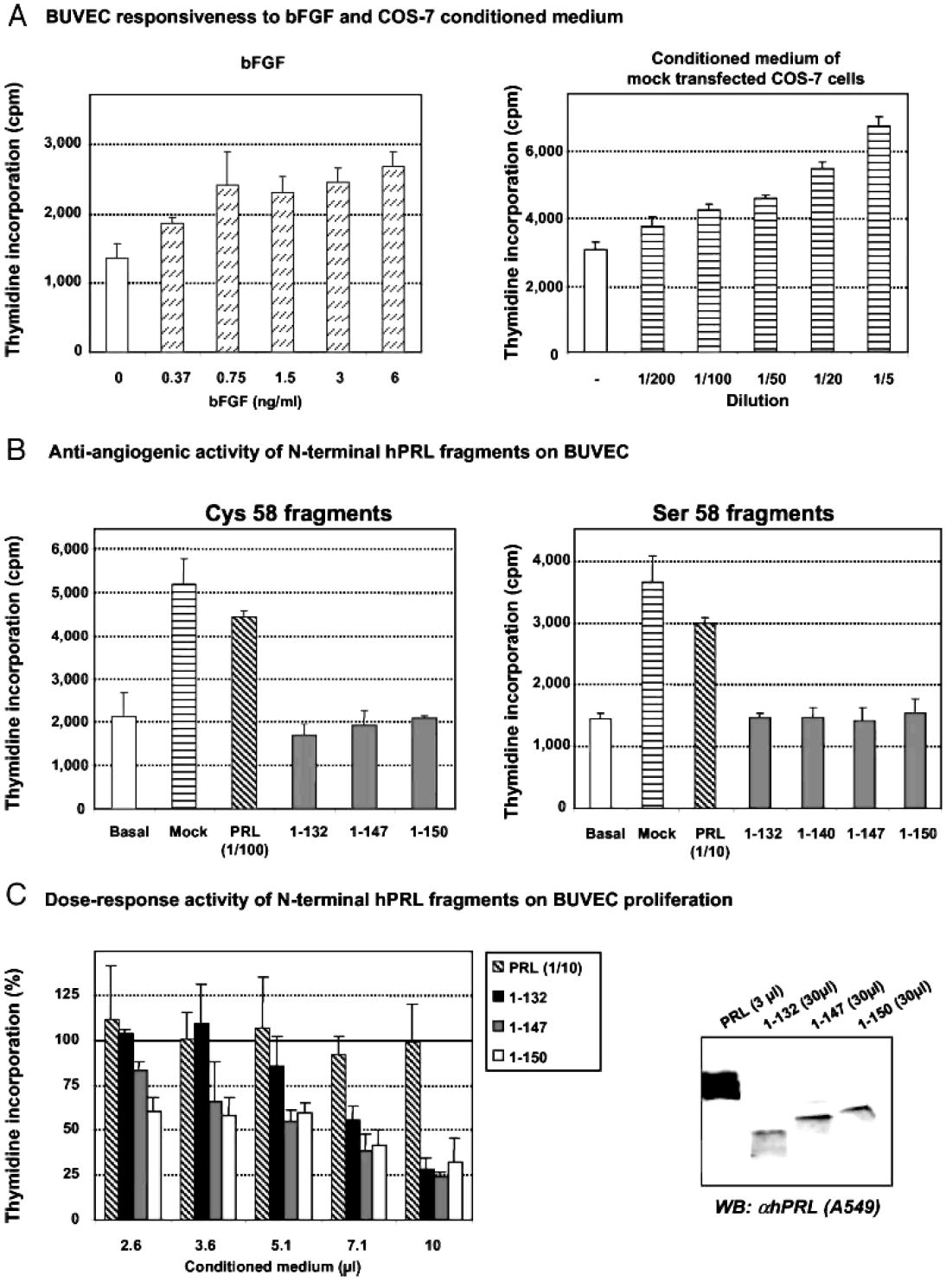

**Figure 7:** *Continued*

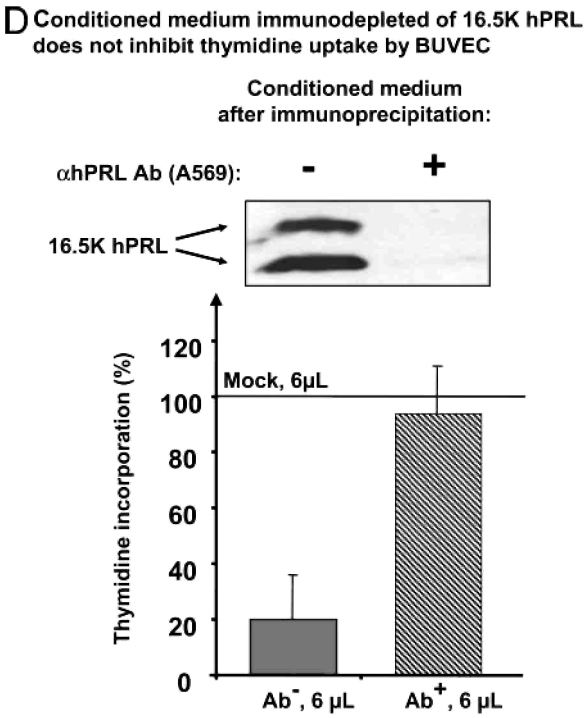


**Antiangiogenic Effect of N-Terminal hPRL Fragments on Endothelial Cells**

The antiangiogenic activity of hPRL fragments secreted from COS-7 cells was determined using immortalized bovine umbilical vein endothelial cells (BUVEC) the growth factor-induced proliferation of which was recently shown to be affected by the addition of 16K rPRL (29). Preliminary studies were performed to ensure the dose-dependent responsiveness of BUVEC to bFGF (Fig. 7A, *left panel*). Because hPRL fragments to be tested were obtained from COS-7 conditioned medium, control experiments were performed to detect any intrinsic effect of culture medium conditioned for 24 h in parental or mock transfected COS-7 cells. As shown on Fig. 7A (*right panel*), conditioned media stimulated the proliferation of BUVEC in a dose-dependent manner, suggesting that COS-7 cells secrete angiogenic factors. Identification of some of these factors was performed using a human angio-genesis antibody array, on which antibodies directed against 20 factors well known to play a role in angiogenic process, are spotted. Membrane incubated in DMEM-0.1% BSA that was used to generate conditioned media served as the negative control. As shown in Fig. 6C, COS-7 cells secrete at least five angiogenesis-related factors that could be specifically distinguished from background in this type of assay: bFGF, VEGF, monocyte chemotactic protein (MCP)-1 and growth-related oncogene (GRO), which are inducers of angiogenesis (30-33), and tissue inhibitor of metalloproteinase (TIMP)-2, which is an inhibitor of angiogenesis (34). The pattern of factors secreted by COS-7 cells was not affected by expression of hPRL fragments (data not shown). To the best of our knowledge, this is the first report identifying angiogenesis-related factors secreted by this cell line. With the exception of VEGF and bFGF, which were shown to stimulate BUVEC proliferation (29), we are not aware of any study that has investigated whether MCP-1, GRO, or TIMP-2 affects BUVEC proliferation *in vitro*, or whether these cells express the cognate receptors of these factors. Such analyses fall beyond the scope of this study and do not question the final effect of COS-7 cell-conditioned medium, which is clearly stimulatory, on BUVEC (Fig. 7A).

Although exogenous bFGF and conditioned medium had an additive effect (data not shown), we omitted adding bFGF in all further bioassays, because angiogenic factors present in COS-7 cell-conditioned medium were sufficient to induce a significant response of BUVEC (>2-fold increase in thymidine uptake over basal). Whether a serine was substituted for the free $Cys_{58}$ or not, 10 $\mu$l of conditioned medium (in 200 $\mu$l final volume) containing any N-terminal hPRL fragment were sufficient to inhibit thymidine uptake induced by mock conditioned medium (Fig. 7B). In some experiments (Fig. 7B), but not all (Fig. 7C), hPRL exhibited a small inhibitory effect that never exceeded 25%, and this was not correlated to the dilution factor. Similar observations have been reported previously (25). We next performed dose-response analyses to better characterize the inhibitory effect of hPRL fragments. Due to the intrinsic angiogenic activity of conditioned media, dose-response bioassays analyses were systematically performed using equivalent volumes of conditioned medium in

each well (*i.e.* hormone-containing conditioned media were normalized with mock transfection conditioned medium). As shown in Fig. 7C, the inhibitory effect of 16K-like fragments was dose dependent, with $IC_{50}$ values in the range of 0.5-1 nM, based on fragment quantification from immunoblots. Due to the lack of real quantitative assay (ELISA) for the fragments, it would be misleading to attempt to predict a more precise $IC_{50}$ value, or to evaluate whether one fragment is slightly more potent than another. Finally, to definitely confirm the specificity of the effect induced by hPRL fragments, we removed 16.5K hPRL from conditioned medium by an immunodepletion experiment. As shown in Fig. 7D, there was no more inhibitory effect on BUVEC in the absence of hPRL fragment. In addition, because the level of thymidine uptake induced by immunodepleted conditioned medium (*right bar*) is similar to that induced by control mock-transfected medium (100% on y-axis), this confirms that the inhibition induced by 16.5K hPRL (*left bar*) is actually fragment dependent and does not result from any loss of activity of the angiogenic factors after the immunoprecipitation procedure.

Thus, hPRL fragments encompassing sequences 1-132 to 1-150, but not full-length PRL, are able to significantly inhibit growth factor-induced thymidine incorporation by BUVEC.

**N-Terminal hPRL Fragments Inhibit Growth Factor-Induced Activation of MAPK**

It was previously shown that 16K hPRL inhibition of growth factor-activated cell proliferation involves the inhibition of signaling cascades upstream of MAPKs (10). As shown in Fig. 8, growth factors secreted by COS-7 cells (mock transfection-conditioned medium) induced rapid phosphorylation of MAPKs (30 min). Full-length hPRL did not markedly affect the level of MAPK phosphorylation. In contrast, it was inhibited by the N-terminal hPRL fragment (16.5K hPRL), and this occurred in a dose-dependent manner. Densitometric analysis of four separate experiments showed that at a 1:20 dilution, this fragment inhibits MAPK activation by more than 75%.

**N-Terminal hPRL Fragments Are Detected in hPRL-Secreting Pituitary Adenomas**

The next and final question addressed in this study relates to the potential physiological relevance of the N-terminal hPRL fragments identified *in vitro.* Before analyzing human samples, we performed epitope mapping of several anti-hPRL monoclonal antibodies available in our laboratory, purchased commercially or obtained from collaborators. We used the following antigenic sequences: full-length hPRL, Δ1-9-hPRL (lacking the nine N-terminal residues), the 15 and 16.5/ 17K N-terminal hPRL fragments generated by cathep-sin D proteolysis, and the 16K C-terminal hPRL fragment obtained after thrombin digestion (18). As shown in Fig. 9A, the three monoclonal antibodies distinguished different regions within hPRL. The mAb 6E4 recognized all the antigens tested, indicating its epitope lies within an overlapping sequence, identified as residues 54-132 (Fig. 9B). In contrast, mAb 5602 maps the N-terminal residues as it fails to detect Δ1-9-hPRL and the C-terminal 16K fragment generated by thrombin, whereas it detects WT hPRL and its N-terminal fragments. Finally, mAb 5601 maps a sequence between residues 151 and 199, because it detects hPRL, Δ1-9-hPRL, and the C-terminal 16K fragment, but none of the N-terminal fragments. Results of the epitope mapping are summarized in Fig. 9B.

These antibodies were used to analyze hPRL-related products present in human pituitary. PRL-secreting adenomas were used to increase the chances of detecting hPRL fragments. Nonsecreting pituitary adenomas were taken as negative controls. Pituitary lysates were immunoprecipitated using mAb 6E4 (which recognizes all the antigens of interest), and then immunoblots using each of the three mAbs were performed in parallel (Fig. 9A). As would be expected, 23-kDa hPRL was the most abundant protein detected in the three PRL-secreting adenomas that could be analyzed, whatever the mAb used for immunoblotting (Fig. 9, *middle panels*). The band comigrating with hPRL (~25 kDa) in the nonsecreting adenoma was identified as the light chain of mAb 6E4 used for immunoprecipitation, because it disappeared when polyclonal A549 antibody was used for immunoblotting (data not shown). In PRL-secreting samples, but not in nonsecreting adenoma, one faster-migrating band was detected using mAb 5602 and mAb 6E4, but not mAb 5601. This immunoreactive band is clearly a hPRL-related product, because 1) it is detected using two different anti-hPRL mAbs mapping distinct epitopes, 2) it is not detected when mAb 6E4 is omitted in the immunoprecipitation (sample no. 3/-Ab), and 3) it is also absent in non-PRL-secreting adenoma. More importantly, the fact that this band is detected using mAb 5602 but not mAb 5601 clearly indicates that it corresponds to an N-terminal, and not a C-terminal, fragment of hPRL. To evaluate whether this N-terminal hPRL fragment corresponds to any of those identified *in vitro*, one of the samples (no. 3) was compared with the fragments generated *in vitro* by cathepsin D. *Right panels* in Fig. 9A show that the N-terminal hPRL fragment identified in pituitary adenomas comigrates with the 17K hPRL, encompassing residues 1-150.

**Fig. 8:** *Activity of N-Terminal Fragments on MAPK Signaling Pathway in BUVEC*

A, Dose-dependent inhibition of growth factor-induced activation of MAPKs by increasing amounts of conditioned medium containing 16.5 KhPRL. The assay (final volume of 200 µl) was performed by stimulating (20 min) BUVEC with COS-7 conditioned medium as indicated (mock, hPRL, or dilutions of 16.5K hPRL). Full-length hPRL containing conditioned medium was diluted 10-fold, as described in the legend to Fig. 7. *B,Bars* represent the level of MAPK phosphorylation averaged from four experiments performed as described in panel A. Densitometric analysis was performed using Kodak 1D 2.0.2 software, and the level of activation induced by mock transfection medium (lane 2 in panel A) was arbitrarily fixed to 100%.

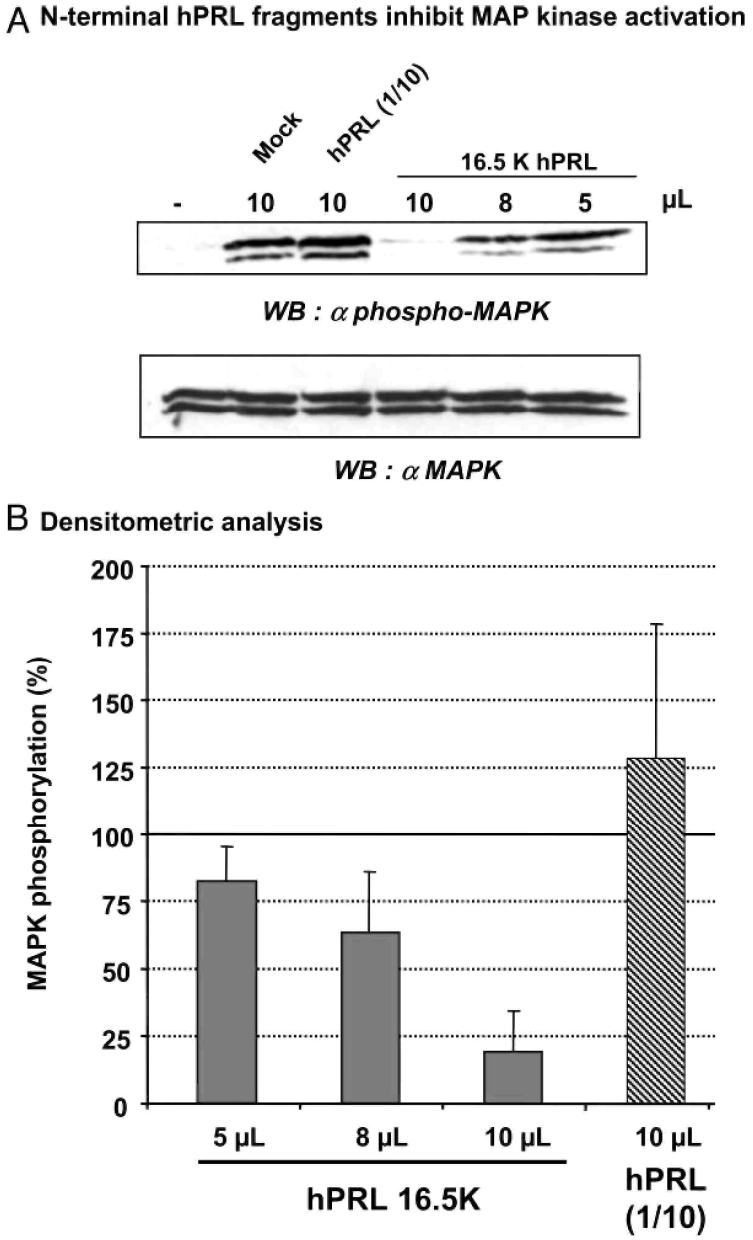

**Fig. 9:** *N-Terminal hPRL Fragments Are Detected in Human Pituitaries*
A, Immunoblot analysis of various hPRL-related products using mAb5602 (fop *blots),* 5601 (*middle blots),* or 6E4 (*bottom blots). Left,* Epitope mapping of the three anti-hPRL monoclonal antibodies was performed using the following hPRL sequences: Δ1-9-hPRL (lane 1), full-length hPRL digested by cathepsin D (lane 2), or thrombin (lane 3). See the text and panel B for interpretation of the results. *Middle,* Three PRL-secreting (nos. 1, 2, and 3) and one nonsecreting (NS) pituitary samples were analyzed after immunoprecipitation with (+Ab) or without (-Ab) mAb 6E4. *, The N-terminal fragment identified in the three PRL-secreting samples. *Right,* The electrophoretic mobility of this N-terminal hPRL fragment is similar to that of 17K hPRL obtained after proteolysis of extractive hPRL by cathepsin D. B, Epitope mapping of the three mAbs as deduced from *left* portions of panel A. Sequences of full-length hPRL and N-terminal and C-terminal fragments are schematically represented by a *horizontal line,* with first and last amino acid indicated. Monoclonal 5602 is directed against the N terminus of hPRL (residues 1-9), whereas mAb 5601 maps a C-terminal epitope, located between residues 150 and 199. Monoclonal 6E4 maps an overlapping epitope between all antigens, located within residues 54 and 133.

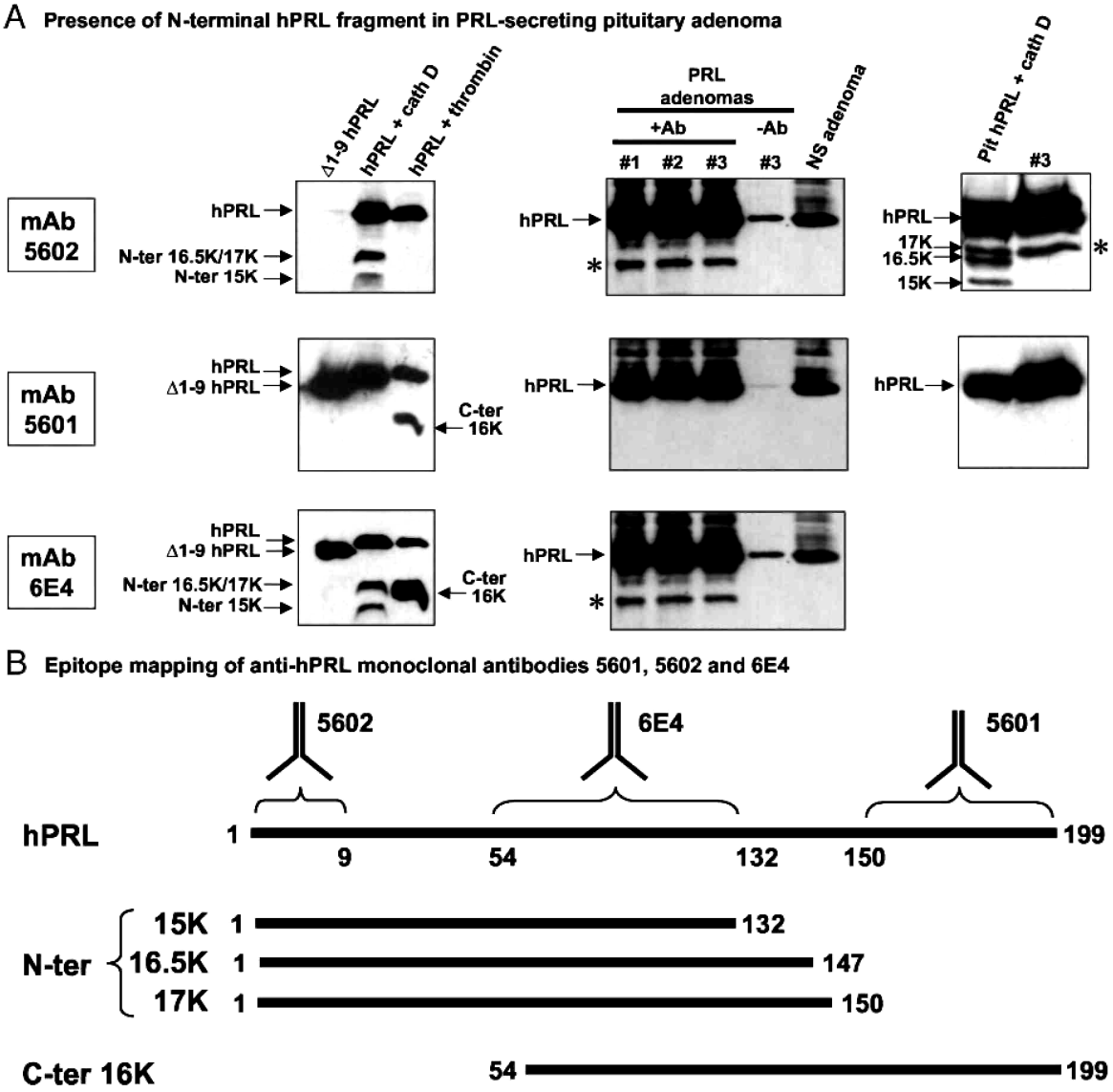


## DISCUSSION

Solid tumor growth is highly dependent on angiogen-esis (35). To remain alive and to divide, cells need oxygen and nutrients, which are transported by the newly formed capillary networks. With the exception of specific physiological conditions, such as menstrual cycle, placenta formation, and tissue repair (wound healing), angiogenesis is a quiescent phenomenon in adults. It is believed that angiogenesis is controlled by a balance between antiangiogenic and proangiogenic factors, the former being predominant in normal conditions, whereas the balance is shifted toward the latter in tumors (36). The antiangiogenic activity of recombinant 16K hPRL has been widely documented in various *in vitro* assays performed on primary endothelial cell cultures (8,9,12), as well as in *in vivo* assays such as the classical angiogenic chick chorioallantoic membrane assay (9). Although the possibility was addressed that the antiangiogenic activity of recombinant 16K PRL could be due, at least in part, to endotoxin contamination of bacterially produced hormones used for the experiments (12), recent data obtained

*in vivo* definitely confirmed the intrinsic antiangiogenic potential of 16K PRL When human colon (25) or prostate (26) cancer cells transfected by expression vectors or infected by adenoviruses encoding 16K hPRL were xe-nografted into athymic mice, their proliferation was markedly inhibited, and this effect could not be mediated by endotoxin contamination because the hormone fragment was expressed by cancer cells themselves.

Although the bioactivity of recombinant N-terminal 16K hPRL is very interesting in a pharmacological context, its putative physiological relevance was recently questioned by the group of Ben-Jonathan (18). Indeed, these authors suggested that no antiangiogenic 16K-like N-terminal fragment could be obtained from proteolysis of hPRL by MCF-7 microsomal pellets, even at acidic pH. In particular, they reported that hPRL is resistant to cathepsin D, which is the protease that was previously shown to cleave rPRL into the antiangiogenic N-terminal 16K fragment (4). In contrast, hPRL undergoes thrombin-mediated processing at physiological pH, also leading to a 16K fragment, but the latter corresponds to the C-terminal sequence of PRL and is completely devoid of any angiostatic activity (18). We herein present data clearly showing that hPRL can be processed *in vitro* into 16K-like N-terminal fragments in experimental conditions identical to those leading to the generation of rat 16K PRL. Obviously, the cleavage efficiency is lower compared with the rat hormone, which may be the reason why it was missed before. We provide several experimental observations arguing that cathepsin D is the protease involved in hPRL processing, the most important being that proteolytic fragments generated by mammary cell lysates or purified cathepsin D displayed the same N-terminal end. Cathepsin D is very abundant in human mammary epithelial cells (37), and its identification as the protease responsible for hPRL cleavage by breast cell extracts or conditioned medium is therefore not surprising. Interestingly, this protease was also shown to be responsible for the generation of another antiangiogenic factor, namely angiostatin, resulting from plasminogen processing (38).

rPRL was shown to contain two cleavage sites for cathepsin D (between residues 145-146 and 148-149) (5, 39), both of which are homologous to cleavage sites that we identified in hPRL (residues 147-148 and 150-151). We demonstrate that the presence of Pro.,$_{48}$ in the hPRL sequence is a limiting factor in the proteolysis, because its removal dramatically increases cleavage efficiency of hPRL, whereas its introduction into the rat sequence has the opposite effect. Two additional cleavage sites were identified in the human hormone. The one between residues 132 and 133 is obviously due to the presence of a Leu at position 132 instead of a Lys in the rat sequence. Although there is no consensus site reported for cathepsin D, these finding are in good agreement with the fact that the introduction of lysine and proline residues within sequences normally recognized by this protease is detrimental to cleavage efficiency (40). Accordingly, the proteolytic patterns obtained for ovine and human PRL are very similar, and distinct from that obtained with rodent PRLs (2), which correlates with the presence of a conserved Pro$_{148}$ in the former and a conserved Lys.,32 in the latter. Finally, a fourth cleavage site was identified in hPRL around residue 85, although its precise location could not be determined because multiple fragments ending between residues 80-85 or starting between residues 85-90 were identified by mass spectrometry. Analysis of the three-dimensional structure of hPRL (41) clearly showed that the four cathepsin D sites are located in the same region of the folded protein and are indeed located very near to each other (Fig. 3D). Sites involving residues 147-148 and 150-151 are located in the large loop linking helices 3 and 4, which is floating on the side of a four-helix bundle and is presumably easily accessible to the protease. The two other sites (132-133 and putative 85-86) are located within helical regions, respectively: the end of helix 3 and beginning of helix 2. Remarkably, the addition of 0.05% Triton X-100 strongly favored proteolysis between residues 132-133, indicating that hPRL intrinsically contains a stretch of amino acids that is highly sensitive to ca-thepsin D. This is reminiscent of the previous observation that nonionic detergents markedly enhanced rPRL proteolysis by kallikrein, a trypsin-like serine protease (42). Under native conditions, the 132-133 proteolytic site is buried inside the protein (Fig. 3D) (41), which probably explains the moderate cleavage; in contrast, the detergent is anticipated to slightly relax hPRL folding, leading to increased accessibility of residues 132-133 and near total cleavage. Although these experiments were aimed only at investigating any relationships between hPRL conformation and proteolytic sensitivity, one may speculate that if hPRL cleavage occurs within the secretory pathway (27), the pattern of fragments generated could depend on its folding state. The antiangiogenic activity of the three 16K-like N-terminal fragments identified in this study was assessed using immortalized BUVEC, which were recently shown to maintain the characteristic features of endothelial cells (29). All N-terminal hPRL fragments produced by COS-7 cells were able to inhibit growth factor-induced thymidine incorporation by BUVEC. Immunodepletion experiments confirmed that the inhibitory effect is totally dependent on the presence of hPRL fragments, because their removal from conditioned medium fully restored the stimulatory effect obtained with mock-transfected medium. Whether the reduction in thymidine uptake strictly reflects an effect on cell proliferation, or also takes into account an increase of cell apoptosis (12,13) or other effects such as reduced cell adhesion, is currently under study in our laboratory. The $IC_{50}$ of this inhibitory action was in good agreement with former studies involving bacte-rially produced 16K hPRL (residues 1-139), which was shown to inhibit the proliferation of bovine brain capillary endothelial cells (9) and neovascularization in the chick chorioallantoic membrane assay (25) with an $IC_{50}$ of 1-2 nM. This demonstrates that eukaryotic cells express correctly folded

hPRL fragments that are at least as potent as those obtained from bacteria, confirming previous observations (25, 43). Even more interesting is the following observation: whereas we previously noticed that some batches of bacterially produced 16K hPRL display weak or, at worst, no antiangiogenic activity, which remains unexplained, we never made such an observation with hPRL fragments secreted by COS-7. As bacterially produced 16K hPRL requires a denaturation-renaturation step that is not needed when using conditioned media, we can assume that the latter system leads to a folding process that is more reproducible. The activity of full-length hPRL on BUVEC was either nil or slightly inhibitory, which is reminiscent of previous reports (25). Some cleavage may occur in COS cells, leading to the generation of small amounts of active 16K hPRL. The presence of a 16K-like band under reducing conditions (Fig. 6A) may argue for this hypothesis, although this remains speculative at this time. At the signaling level, the antiproliferative activity of 16K PRL was shown to involve inhibition of cascades upstream of MAPK activation (10, 11). Accordingly, the hPRL fragments identified in this study were able to inhibit the phosphorylation of MAPKs induced by growth factors, and this was also dose dependent as shown for 16.5K hPRL

From a sequence-function point of view, the activity of 15K hPRL (1-132) is not surprising because previous studies showed that hPRL fragments slightly shorter (residues 1-123) (8) or longer (residues 1-139) (Ref. 9 and this study) displayed antiangiogenic activity. Similarly, the length of the two larger fragments (1-147 and 1-150) is almost the same as that of 16K rPRL (1-145), which is also antiangiogenic in the assay used in the present work (29). Although these data confirm that C-terminal truncation of hPRL by not more than one quarter of its sequence (49 amino acids) is sufficient to convert the lactogenic hormone PRL into an antiangiogenic factor, they also emphasize our current ignorance of the molecular features driving 16K PRL properties. Functional analysis of N-terminal hPRL fragments longer than 150 residues and shorter than 123 will lead to a better understanding of the structure-function requirements of 16K-like PRL fragments. Finally, our functional studies were performed using highly glycosylated hPRL fragments. The antiangiogenic properties of bacterially-produced 16K hPRL do not support any key role for glycosylation, although we cannot exclude the possibility that this modification modulates the biological properties of our recombinant fragments. Testing this hypothesis would involve mutation of the single glycosylation site present in hPRL sequence, Asn 31 (44).

Data currently available in the literature concerning human 16K PRL raise a paradox. Although several investigators published important studies describing the antiangiogenic activity of recombinant 16K hPRL in various models as well as certain molecular mechanisms involved (see *Introduction)*, we are not aware of any report in which the existence of similar N-terminal 16K hPRL *in vivo* has been clearly demonstrated. A few reports have appeared showing that 14-18 kDa immunoreactive bands were detected when physiological fluids, tissue extracts, or cell culture-conditioned media were analyzed under reducing SDS-PAGE, followed by Western blotting experiments using polyclonal or monoclonal anti-PRL antibodies (45-49)(for a review, see Ref. 3). However, in most of these studies, immunoreactive bands were not clearly demonstrated to be PRL related, and assuming they were, their identification as N-terminal PRL fragments was not assessed using appropriate methods (epitope-mapped mAb, N-terminal sequencing, mass spectrometry). This clearly prevents any definite statement regarding the relevance of antiangio-genic 16K PRL in humans, because the recent work of Ben-Jonathan and colleagues (18) tends to suggest that these immunoreactive bands may rather correspond to C-terminal 16K hPRL, which has no angio-static activity. In this context, our analyses of human pituitary adenomas provide an important information, because the use of epitope-mapped mAbs clearly identified the immunoreactive 16K-like band as an N-terminal hPRL fragment. Based on the comparison with the *in vitro* digestion pattern of hPRL, the fragment observed in pituitaries matches with 17K hPRL. Assuming that cathepsin D is the pituitary protease involved, which remains to be definitely demonstrated, this suggests that the 150-151 site would be the preferential cleavage site *in vivo.* The fact that 15K and 16.5K fragments could not be detected is in good agreement with the observations that 1) the 132-133 site is buried inside hPRL, and 2) $Pro_{148}$ is detrimental to cleavage efficiency. Finally, because it is likely that the presence of 17K hPRL in PRL-secreting, but not in nonsecreting, adenomas is primarily due to the fact that overexpression of hPRL in the former favors the detection of proteolytic fragments present in small amounts, it is probably misleading at this stage to link the presence of hPRL fragments with the pathological characteristics of the tumor.

We showed that recombinant 17K hPRL displayed antiangiogenic bioactivity, even when free $Cys_{58}$ is maintained, which is obviously the case for the 17K fragment detected in pituitaries. Therefore, our study certainly renews the interest in the potential relevance of antiangiogenic N-terminal PRL fragments in humans. Many questions remain answered, however, which prevent definitive interpretations. First, to facilitate the detection of fragments assumed to be present in relatively low amounts, we used PRL-secreting pituitary adenomas. Similar experiments should now be performed using nonpathological samples (e.g. serum, breast biopsies, etc), to elucidate whether the presence of hPRL N-terminal fragments is correlated with any pathological status or not. Such investigations will be possible once sensitive antibodies specifically directed

against hPRL fragments are available; this is an ongoing project in our laboratory. Second, although the fragment detected in pituitary adenomas matches 17K hPRL, analysis of additional samples is required to determine whether other fragments, possibly generated by other proteases, can be identified. Third, it is noteworthy that in all the experiments reported in this study, including pituitary analyses, N-terminal fragments were detected only when electrophoreses were performed under reducing conditions. As described in the *Introduction*, the release of 16K PRL requires proteolytic cleavage followed by reduction of the cleaved hormone. The molecular and cellular mechanisms that may lead to reduction of cleaved PRL *in vivo* are currently unknown, irrespective of the species considered. Understanding this process, or demonstrating that N-terminal 16K-like fragments can be detected in human samples under nonreducing conditions, is certainly a goal that must be obtained in the future.

If proteolysis and reduction occur in the mammary gland *in vivo*, our findings may be important for better understanding the role of PRL in breast carcinogenesis, which is a major goal of our group. Cathepsin D is expressed at a high level in breast cancer (37) and could therefore play a key role in regulating the release of cryptic antiangiogenic factors, e.g. 16K-like hPRL and angiostatin. In addition, recent observations suggest that locally produced hPRL participates in the growth of mammary tumors via an autocrine/paracrine loop (17). Autocrine hPRL thus might be very important in tumor progression, especially in view of its putative angiogenic action described in the chorioallantoic membrane assay (13). The present study suggests that the protumor action of hPRL in mammary tumorigenesis may be balanced by the antiangiogenic activity of N-terminal 16K-like hPRL fragments. Confirming the relevance of this model will require demonstrating how and where the molecular and cellular features leading to PRL processing into 16K PRL (protease, acidic pH, reductase, *etc.*) occur *in vivo.*

## MATERIALS AND METHODS

### Materials

### Reagents and Culture Media.

Salts were high-grade purified chemicals purchased from Sigma Chemical Co. (St. Louis, MO) or Merck (Darmstadt, Germany). Oligonucleotides were from Eurogentec (Liege, Belgium). Culture media, fetal calf serum (FCS), trypsin, and glutamine were purchased from Life Technologies, Inc. (Gaithersburg, MD). [$^{3}$H]thymidine was purchased from Amersham (Buckinghamshire, UK).

### Proteins and Antibodies.

For digestion studies, we used recombinant human and rat PRL produced in bacteria (pT7L-PRL vector) and purified as previously reported (21). Mutated hPRL and rPRL generated in this study were produced following exactly the same procedures. Extractive hPRL (lot 120-16-2) was a generous gift of Dr. Parlow (National Institute of Diabetes and Digestive and Kidney Diseases; NHPP no. 506). BSA was from Sigma. Anti-hPRL mAb (mAb clone 6E4) is directed against a recombinant N-terminal fragment (residues 1-139) of hPRL (14). 6E4 mAb was found to recognize both full-length and N-terminal fragments of hPRL in Western blots. Polyclonal anti-hPRL antibody A569 was purchased from DAKO Corp. (Carpinteria, CA), and mAb 5601 and 5602 are from DBC (Diagnostic Biochem Canada, Inc., London, Ontario, Canada). Extractive human liver cathepsin D, human plasma thrombin, and protease inhibitors were from Sigma. Antihuman cathepsin D mAb was a gift from Dr M. Garcia (INSERM Unit 540, France), and glycosidase (*N*-glycosidase F) was from New England Biolabs, Inc. (Beverly, MA). Monoclonal antiactive MAPK antibody (directed against threonine202/tyrosine204-phosphorylated MAPKs 1 and 2 (no. 9106), also referred to as antiactive Erk 1/2) was from Cell Signaling Technology (Beverly, MA) and polyclonal anti-MAPK1/2 antibody (no. 06-182) was from Upstate Biotechnology, Inc. (Lake Placid, NY). Quantification of 23-kDa hPRL secreted by COS-7 into cell-conditioned media was performed using a hPRL-specific ELISA (Prolactin Elisa kit, DBC). Identification of angiogenic factors secreted by COS-7 cells was performed using human angiogenesis antibody arrays I purchased from RayBiotech, Inc. (Norcross, GA). For both Prolactin Elisa kit and angiogenesis array, we strictly followed the instructions of the manufacturers.

### Cell Lines and Human Mammary Biopsies.

Tumor breast biopsies were obtained from three patients bearing a breast cancer, as previously described (50). Normal tissue adjacent to the tumor was also harvested during surgery. T-47Dco cells, an estrogen-resistant clone of the T-47D human breast adenocarcinoma cell line (51), were obtained from Dr. B. K. Vonderhaar

(National Institutes of Health, Be-thesda, MD). They were routinely cultured in RPMI 1640 supplemented with 10% FCS, L-glutamine (2 mM), insulin (0.2 IU/ml), and antibiotics. Immortalized BUVEC were generated by transfecting primary cell cultures with an expression vector containing the human papillomavirus type 16 E6E7 oncogene as previously described (29). They were routinely cultured in F12-K, 10% FCS, glutamine, and antibiotics. COS-7 cells were routinely cultured in DMEM, 10% FCS, glutamine, and antibiotics.

**Pituitary Adenomas.**

Pituitary samples were collected in patients undergoing surgical adenomectomy at Hδpital Foch (Paris, France). Both PRL-secreting and nonsecreting adenomas were made available for this study. Directly after their removal, pituitary samples were snap frozen until use.

**Methods**

**Site-Directed Mutagenesis and Expression Plasmids.**

Expression vectors for N-terminal fragments of hPRL were generated by introducing a stop codon within the hPRL coding sequence subcloned into the pc-DNA3.1 vector (Invitro-gen, San Diego, CA). Site-directed mutagenesis was performed using the QuikChange Mutagenesis kit from Stratagene (La Jolla, CA). A stop codon was substituted for codons 133, 148, or 151, leading to hPRL fragments of approximately 15 kDa (1-132), 16.5 kDa (1-147), and 17 kDa (1-150), respectively. Cognate mutants in which a serine is substituted for cysteine 58 were also generated and are referred to as C58S analogs. The plasmid encoding the 1-139 fragment of hPRL was generated previously (9) and is identified in this study as 16K hPRL.

**Cleavage of hPRL by Cell Extracts, Cell-Conditioned Medium, or Purified Cathepsin D.**

Mammary cell homogenates were prepared from T-47Dco cells and pulverized breast tissues as described elsewhere (52). Briefly, cells were placed in 7.5 vol (wt/vol) of ice-cold 0.25 M sucrose/0.1 M Tris-HCl (pH 7.4), and homogenized for 30 sec using a Polytron homogenizer. The high-speed sediment was obtained by three successive centrifugations (10 min each) at 600 x *g*, 3,300 x *g*, and 25,000 x *g*. The final pellet was washed twice in the same buffer.

Fifty micrograms of the 25,000 x *g* pellet were incubated with 20 μg hPRL for the indicated time at room temperature, in a final volume of 25 μl of 50 mM citrate-phosphate/75 mM NaCl (pH 3.2) (2). Heat-inactivated pellets (85 C, 30 min) were used as negative controls. Proteolysis was also performed using culture medium conditioned for 24 h with T-47Dco cells, and then acidified (pH 3.2) using HCl. Negative controls were either acidified nonconditioned medium or nonacidified conditioned medium (pH ~7). Various protease inhibitors were used at the following concentration: pepstatin A (1 μM), leupeptin (100 μM), aprotinin (0.3 μM), phenylmethylsulfonyl fluoride (0.2 mM), EDTA (5 mM). Proteolysis of hPRL (20 μg) by purified cathepsin D was performed for the indicated time, at room temperature or at 37 C, in 20 mM citrate/phosphate, 150 mM NaCI (pH 3 or 7) (4), using an enzyme-substrate ratio of 1:100.

**Analysis of Pituitary Adenomas.**

Pituitary adenoma samples were thawed on ice, washed several times in ice-cold PBS to remove blood and tissue debris, and then homogenized using a Polytron, in lysis buffer containing various protease inhibitors as previously described (53). Tissue homogenates were centrifuged at 10,000 x *g* for 10 min, and the pellet was discarded. For immunoprecipitation experiments, 500 μg of the tissue lysate proteins were precleared by incubation with protein A-sepharose beads for 2 h at 4 C. Protein A-sepharose beads were removed by brief centrifu-gation, and then supernatants were transferred to fresh tubes. Immunoprecipitations were performed by incubating lysates with 5 μl of mAb 6E4, overnight at 4 C. Immunocomplexes were collected by adding protein A-sepharose beads for 1 h. Immunoprecipitates were washed three times with PBS before loading on SDS-PAGE.

**SDS-PAGE and Immunoblots.**

Analysis of PRL fragments was performed using 15-17% SDS-PAGE, in reducing and nonreducing conditions as indicated. Gels were either stained with Coomassie blue or immunoblotted using the following anti-hPRL antibodies: mAb 6E4 (2 μg/ml), polyclonal A569 (1:500 dilution), mAb 5601 or mAb 5602 (1:40 dilution). Antigen-antibody complexes were detected by enhanced chemiluminescence (Amersham) using an antimouse or

antirabbit immunoglobulin antibody conjugated to horseradish peroxidase.

**N-Terminal Sequencing of hPRL Fragments.**

hPRL fragments resulting from proteolysis by mammary cell extracts or by purified cathepsin D were separated by reducing SDS-PAGE and transferred onto a polyvinylidene difluoride membrane using 10 mM (3-[cyclohexylamino]-1-propane-sulfonic acid) buffer from Sigma (pH 10.5). Bands were visualized by Ponceau red staining and cut out of the gel, and N-terminal sequences were determined by Edman degradation (Laboratory of Biochemistry, University of Liege, Liege, Belgium).

**Mass Spectrometry.**

hPRL (10 µg) [WT, or analogs referred to as Δ1-9-hPRL and G129R-hPRL (22, 28)] were digested by cathepsin D (3 h) in a final volume of 25 µl citrate/phosphate buffer as described above. Oxidized and reduced (100 mM dithiothreitol) hormone mixtures were then analyzed by mass spectrometry. Typically, 1 µl of nondi-gested or digested protein was mixed with 1 µl of matrix (sinapinic acid, 7.5 mg in 500 µl acetonitrile:$H_2O$-0.1 % trifluoroacetic acid, 1:1 vol/vol) and 1 µl was deposited on the sample holder. Positive ions mass spectra were acquired on a MALDI-TOF Voyager Elite (Applied Biosystems, Framing-ham, MA) in the linear mode using the delayed extraction. Internal and external calibration were performed using apo-myoglobin [singly and doubly protonated molecules $(M + H)^+$ and $(M+2H)^{2+}$]. Uncertainties on the m/z values were determined from the analysis of different samples. Experiments on electroblotted (nitrocellulose) proteins (full length and fragments) were performed by dissolving approximately 1 $mm^2$ of the band in the matrix solution (solvent acetone), but the mass spectra showed broader peaks. Thus, only the results concerning the MALDI-TOF of solutions are presented.

**Production of N-Terminal Fragments of hPRL in COS Cells.**

COS-7 cells were transiently transfected using lipo-fectamine plus (Invitrogen), using the following expression vectors: pcDNA3.1 vector (mock transfection), vectors encoding full-length hPRL, fragments encompassing sequences 1-132 (15K), 1-147 (16.5K), 1-150 (17K), in which the free cysteine 58 is maintained or replaced with a serine (C58S analogs), and finally the reference construct 1-139 (16KhPRL-C58S).

For transfections, cells were plated in six-well plates (200,000 cells per well) in 10% FCS medium (d 1). On d 2, cells were transfected using 1 µg plasmid in 4 µl lipo-fectamine/6 µl plus reagent; we strictly followed the instructions of the manufacturer. On d 3, cells were serum starved in DMEM/0.1 % BSA, and conditioned media were harvested on d 4. Expression of hormones of interest was checked by Western blotting. Analytical deglycosylation of recombinant hPRL fragments was performed using F glycosidase by strictly following the instructions of the manufacturer.

**Immunodepletion of COS-7-Conditioned Media.**

Conditioned media (100 µl) containing hPRL fragment were incubated overnight at 4 C with 1 µl of polyclonal anti-hPRL antibody (A569). Protein A sepharose beads (20 µl) were incubated in the immunoprecipitation mixture for one additional hour, and then immune complexes were removed by brief centrifugation. Both the pellet and the supernatant were analyzed in Western blot to assess withdrawal of hPRL fragments from the conditioned medium.

**Biological Properties of N-Terminal hPRL Fragments**

**Tritiated Thymidine Incorporation.**

Antiangiogenic properties of N-terminal hPRL fragments were determined using immortalized BUVEC, which were recently shown to retain a differentiated phenotype and all the characteristics of endothelial cells and to maintain their responsiveness to rat 16K PRL (29). Cells were serum-starved in the flasks 24 h before the assay and were then plated in 48-well plates (8000 cells per well; each point in triplicate) in 100 µl of F-12K containing 0.2% FCS. Stimulation by the hormones of interest was performed by adding 100 µl of serum-free DMEM containing the indicated dilution of COS-7-conditioned media, either the same day or the day after. Because COS-7-conditioned medium intrinsically stimulated thymidine incorporation by BUVEC, various dilutions of conditioned media containing PRL fragments were systematically normalized to the same volume using mock-transfected conditioned medium (see *Results*). After stimulation (16-18 h), cells were pulsed for 4 h

with [$^3$H]thymidine (0.5 $\mu$Ci/well), and then they were treated as previously described with minor modifications (25). Incorporated radioactivity was measured using a liquid scintillation counter (Wallaw 1409).

**MAPK Activation.**

BUVEC were plated in 10% FCS medium on d 1, serum starved on d 2, and stimulated on d 3 with the various PRLs (in serum-free medium) for 20 min. Cells were harvested and lyzed as previously described (53). Analyses of MAPK activation were performed using 20 $\mu$g of total cell lysates, by SDS-PAGE (12.5%) followed by Western blotting using antiphosphorylated MAPK antibody (dilution 1:2000). After stripping, membranes were reprobed using anti-MAPK antibody (dilution 1:2000).

## ACKNOWLEDGMENTS

We are grateful to Dr. M. Garcia for providing anticathepsin D antibodies, to Dr. R. Schijns for help with peptide sequencing experiments, and to Drs. A. Visot and S. Jourdain (Hôpital Foch, Paris, France) for providing pituitary samples. C. Kay-ser and C. Burie are acknowledged for technical assistance. We thank Dr. Bernadette Arnoux for generating Fig. 3D, and F. Dubail for help with circular dichroism analyses.

This work was supported in part by INSERM, the Comité de Paris de la Ligue Nationale contre le Cancer, Fortis Bank, and the Conseil de la Recherche et du Développement de L'Université de Liège (fonds spéciaux). D.P. is supported by a student fellowship from the Ministry of Research and Technology of France, ST. by FRIA ("Fond pour la Recherche Industrielle et Agricole"), and I.S. by FNRS ("Fonds National de la Recherche Scientifique").

## REFERENCES

1. Clapp C, Sears PS, Russell DH, Richards J, Levay-Young BK, Nicoll CS 1988 Biological and immunological characterization of cleaved and 16K forms of rat prolactin. Endocrinology 122:2892-2898

2. Clapp C 1987 Analysis of the proteolytic cleavage of prolactin by the mammary gland and liver of the rat: characterization of the cleaved and 16K forms. Endocrinology 121:2055-2064

3. Corbacho AM, las Escalera GM, Clapp C 2002 Roles of prolactin and related members of the prolactin/growth hormone/placental lactogen family in angiogenesis. J Endocrinol 173:219-238

4. Baldocchi RA, Tan L, King DS, Nicoll CS 1993 Mass spectrometric analysis of the fragments produced by cleavage and reduction of rat prolactin: evidence that the cleaving enzyme is cathepsin D. Endocrinology 133:935-938

5. Andries M,Tilemans D, Denef C 1992 Isolation of cleaved prolactin variants that stimulate DNA synthesis in specific cell types in rat pituitary cell aggregates in culture. Biochem J 281:393-400

6. Goffin V, Shiverick KT, Kelly PA, Martial JA 1996 Sequence-function relationships within the expanding family of prolactin, growth hormone, placental lactogen and related proteins in mammals. Endocr Rev 17:385-410

7. Cooke NE, Coit D, Shine J, Baxter JD, Martial JA 1981 Human prolactin: cDNA structural analysis and evolutionary comparisons. J Biol Chem 256:4007^016

8. Clapp C, Martial JA, Guzman RC, Rentier-Delrue F, Weiner Rl 1993 The 16-kilodalton N-terminal fragment of human prolactin is a potent inhibitor of angiogenesis. Endocrinology 133:1292-1299

9. Struman I, Bentzien F, Lee H, Mainfroid V, D'Angelo G, Goffin V, Weiner Rl, Martial JA 1999 Opposing actions of intact and N-terminal fragments of the human prolactin/ growth hormone family members on angiogenesis: novel mechanism for the regulation of angiogenesis. Proc Natl Acad Sci USA 96:1246-1251

10. D'Angelo G, Struman I, Martial JA, Weiner Rl 1995 Activation of mitogen-activated protein kinases by vascular endothelial growth factor and basic fibroblasts growth factor in capillary endothelial cells is inhibited by the anti-angiogenic factor 16-kDa N-terminal fragment of prolactin. Proc Natl Acad Sci USA 92:6374-6378

11. D'Angelo G, Martini JF, liri T, Fantl WJ, Martial J, Weiner Rl 1999 16K human prolactin inhibits vascular endothelial growth factor-induced activation of Ras in capillary endothelial cells. Mol Endocrinol 13:692-704

12. Martini JF, Piot C, Humeau LM, Struman I, Martial JA, Weiner Rl 2000 The antiangiogenic factor 16K PRL induces programmed cell death in endothelial cells by caspase activation. Mol Endocrinol 14:1536-1549

13. Tabruyn SP, Sorlet CM, Rentier-Delrue F, Bours V, Weiner Rl, Martial JA, Struman 12003 The antiangiogenic factor 16K human prolactin induces caspase-dependent apoptosis by a mechanism that requires activation of nuclear factor-κB. Mol Endocrinol 17:1815-1823

14. Lee H, Struman I, Clapp C, Martial J, Weiner Rl 1998 Inhibition of urokinase activity by the antiangiogenic factor 16K prolactin: activation of plasminogen activator inhibitor 1 expression. Endocrinology 139:3696-3703

15. Clapp C, Weiner Rl 1992 A specific, high affinity, saturable binding site for the 16-kilodalton fragment of prolactin on capillary endothelial cells. Endocrinology 130: 1380-1386

16. Goffin V, Binart N, Touraine P, Kelly PA 2002 Prolactin: the new biology of an old hormone. Annu Rev Physiol 64:47-67

17. Clevenger CV, Furth PA, Hankinson SE, Schuler LA 2003 The role of prolactin in mammary carcinoma. Endocr Rev 24:1-27

18. Khurana S, Liby K, Buckley AR, Ben-Jonathan N 1999 Proteolysis of human prolactin: resistance to cathepsin D and formation of a nonangiostatic, C-terminal 16K fragment by thrombin. Endocrinology 140:4127^132

19. Baldocchi RA, Tan L, Nicoll CS 1992 Processing of rat prolactin by rat tissue explants and serum *in vitro*. Endocrinology 130:1653-1659

20. Bernichtein S, Jomain JB, Kelly PA, Goffin V 2003 The N-terminus of human prolactin modulates its biological properties. Mol Cell Endocrinol 208:11-21

21. Paris N, Rentier-Delrue F, Defontaine A, Goffin V, Lebrun JJ, Mercier L, Martial JA 1990 Bacterial production and purification of recombinant human prolactin. Biotechnol Appl Biochem 12:436-449

22. Goffin V, Struman I, Mainfroid V, Kinet S, Martial JA 1994 Evidence for a second receptor binding site on human prolactin. J Biol Chem 269:32598-32606

23. Bernichtein S, Jeay S, Vaudry R, Kelly PA, Goffin V 2003 New homologous bioassays for human lactogens show that agonism or antagonism of various analogs is a function of assay sensitivity. Endocrine 20:177-190

24. Volpert O, Luo W, Liu TJ, Estrera VT, Logothetis C, Lin SH 2002 Inhibition of prostate tumor angiogenesis by the tumor suppressor CEACAM1. J Biol Chem 277:35696-35702

25. Bentzien F, Struman I, Martini JF, Martial J, Weiner R 2001 Expression of the antiangiogenic factor 16K hPRL in human HCT116 colon cancer cells inhibits tumor growth in Rag1(-/-) mice. Cancer Res 61:7356-7362

26. Kim J, Luo W, Chen DT, Earley K, Tunstead J, Yu-Lee LY, Lin SH 2003 Antitumor activity of the 16-kDa prolactin fragment in prostate cancer. Cancer Res 63:386-393

27. Dannies PS 1999 Protein hormone storage in secretory granules: mechanisms for concentration and sorting. En-docr Rev 20:3-21

28. Bernichtein S, Kayser C, Dillner K, Moulin S, Kopchick JJ, Martial JA, Norstedt G, Isaksson O, Kelly PA, Goffin V 2003 Development of pure prolactin receptor antagonists. J Biol Chem 278:35988-35999

29. Cajero-Juarez M, Avila B, Ochoa A, Garrido-Guerrero E, Varela-Echavarria A, Martinez D, Clapp C 2002 Immortalization of bovine umbilical vein endothelial cells: a model for the study of vascular endothelium. Eur J Cell Biol 81:1-8

30. Salcedo R, Ponce ML, Young HA, Wasserman K, Ward JM, Kleinman HK, Oppenheim JJ, Murphy WJ 2000 Human endothelial cells express CCR2 and respond to MCP-1: direct role of MCP-1 in angiogenesis and tumor progression. Blood 96:34-40

31. Loukinova E, Dong G, Enamorado-Ayalya I, Thomas GR, Chen Z, Schreiber H, Van Waes C 2000 Growth regulated oncogene-α expression by murine squamous cell carcinoma promotes tumor growth, metastasis, leukocyte infiltration and angiogenesis by a host CXC receptor-2 dependent mechanism. Oncogene 19:3477-3486

32. Ferrara N, Gerber HP, LeCouter J 2003 The biology of VEGF and its receptors. Nat Med 9:669-676

33. Cross MJ, Claesson-Welsh L2001 FGF and VEGF function in angiogenesis: signalling pathways, biological responses and therapeutic inhibition. Trends Pharmacol Sci 22:201-207

34. Seo DW, Li H, Guedez L, Wingfield PT, Diaz T, Salloum R, Wei BY, Stetler-Stevenson WG 2003 TIMP-2 mediated inhibition of angiogenesis: an MMP-independent mechanism. Cell 114:171-180

35. Folkman J 1971 Tumor angiogenesis: therapeutic implications. N Engl J Med 285:1182-1186

36. Hanahan D, Folkman J 1996 Patterns and emerging mechanisms of the angiogenic switch during tumorigenesis. Cell 86:353-364

37. Rochefort H, Liaudet-Coopman E 1999 Cathepsin D in cancer metastasis: a protease and a ligand. APMIS 107:86-95

38. Morikawa W, Yamamoto K, Ishikawa S, Takemoto S, Ono M, Fukushi J, Naito S, Nozaki C, IwanagaS, Kuwano M 2000 Angiostatin generation by cathepsin D secreted by human prostate carcinoma cells. J Biol Chem 275: 38912-38920

39. Baldocchi RA, Tan L, Horn YK, Nicoll CS 1995 Comparison of the ability of normal mouse mammary tissues and mammary adenocarcinoma to cleave rat prolactin. Proc Soc Exp Biol Med 208:283-287

40. Pimenta DC, Oliveira A, Juliano MA, Juliano L2001 Substrate specificity of human cathepsin D using internally quenched fluorescent peptides derived from reactive site loop of kallistatin. Biochim Biophys Acta 1544:113-122

41. Keeler C, Dannies PS, Hodsdon ME 2003 The tertiary structure and backbone dynamics of human prolactin. J Mol Biol 328:1105-1121

42. Powers CA, Hatala MA 1990 Prolactin proteolysis by glandular kallikrein: *in vitro* reaction requirements and cleavage sites, and detection of processed prolactin *in vivo.* Endocrinology 127:1916-1927

43. Galfione M, Luo W, Kim J, Hawke D, Kobayashi R, Clapp C, Yu-Lee LY, Lin SH 2003 Expression and purification of the angiogenesis inhibitor 16-kDa prolactin fragment from insect cells. Protein Expr Purif 28:252-258

44. Sinha YN 1995 Structural variants of prolactin: occurrence and physiological significance. Endocr Rev 16: 354-369

45. Sinha YN, Gilligan TA, Lee DW, Hollingsworth D, Markoff E 1985 Cleaved prolactin: evidence for its occurrence in human pituitary gland and plasma. J Clin Endocrinol Metab 60:239-243

46. Warner MD, Sinha YN, Peabody CA 1993 Growth hormone and prolactin variants in normal subjects. Relative proportions in morning and afternoon samples. Horm Metab Res 25:425-429

47. Fukuoka H, Hamamoto R, Higurashi M 1991 Heterogeneity of serum and amniotic fluid prolactin in humans. Horm Res 35(Suppl 1):58-63

48. Pellegrini I, Gunz G, Ronin C, Fenouillet E, Peyrat JP, Delori P, Jaquet P 1988 Polymorphism of prolactin secreted by human prolactinoma cells: immunological, receptor binding, and biological properties of the glycosylated and non-glycosylated forms. Endocrinology 122:2667-2674

49. Corbacho AM, Macotela Y, Nava G, Tomer L, Duenas Z, Noris G, Morales MA, Martinez De La Escalera G, Clapp C 2000 Human umbilical vein endothelial cells express multiple prolactin isoforms. J Endocrinol 166:53-62

50. Touraine P, Martini JF, Zafrani B, Durand JC, Labaille F, Malet C, Nicolas A, Trivin C, Postel-Vinay MC, Kuttenn F, Kelly PA 1998 Increased expression of prolactin receptor gene assessed by quantitative polymerase chain reaction in human breast tumors *versus* normal breast tissues. J Clin Endocrinol Metab 83:667-674

51. Horwitz KB, Mockus MB, Lessey BA 1982 Variant T47D human breast cancer cells with high progesterone-receptor levels despite estrogen and antiestrogen resistance. Cell 28:633-642

52. Compton MM, Witorsch RJ 1984 Proteolytic degradation and modification of rat prolactin by subcellular fractions of the rat ventral prostate gland. Endocrinology 115: 476-484

53. Llovera M, Pichard C, Bernichtein S, Jeay S, Touraine P, Kelly PA, Goffin V2000 Human prolactin (hPRL) antagonists inhibit hPRL-activated signaling pathways involved in breast cancer cell proliferation. Oncogene 19:4695-4705